1. Report No. FHWA/TX-05/0-4827-2	2. Government Accession No.	3. Recipient's Catalog No.	
4. Title and Subtitle Feasibility Study of Non-Contact, High-Speed Elastic Property Measurement of Pavements		5. Report Date December 2005	
		6. Performing Organization Code	
7. Author(s) Aditya Ekbote, Huichun Xing, Jing Li, Xuemin Chen, and Richard Liu		8. Performing Organization Report No. 0-4827-2	
9. Performing Organization Name and Address Department of Electrical and Computer Engineering University of Houston 4800 Calhoun Rd. Houston, TX 77204-4005		10. Work Unit No.	
		11. Contract or Grant No. Project 0-4827	
12. Sponsoring Agency Name and Address Texas Department of Transportation Research and Technology Implementation Office P. O. Box 5080 Austin, TX 78763-5080		13. Type of Report and Period Covered Technical Report September 2004 – August 2005	
		14. Sponsoring Agency Code	

15. Supplementary Notes
   Project performed in cooperation with the Texas Department of Transportation and the Federal Highway Administration.
   URL: http://tti.tamu.edu/documents/0-4827-2.pdf

16. Abstract:

Elastic properties of asphalt pavements are extensively used for pavement evaluation and maintenance scheduling. Presently, methods such as Falling Weight Deflectometer (FWD), Plate Load Tests and Rolling Dynamic Deflectometer (RDD) are used by the Department of Transportation for these measurements. These methods have a very slow rate of data production because they are contact measurement systems. In this project, a laser system and a Ground Penetrating Radar (GPR) system were developed for measurement of the elastic properties of asphalt pavement. Several experiments and field tests were conducted at highway speeds using the GPR to find the correlation between the electrical properties and elastic properties of asphalt pavements. Lab tests performed using the Frequency Modulated Continuous Wave (FMCW) GPR and the Pulse GPR indicated a close correlation between the dielectric constant of asphalt and its density. The Pulse GPR was then used to estimate pavement deflection for a 0.3 mile pavement section and the results were compared with the FWD results. The pavement deflections estimated using the GPR and those measured using the FWD were found to be within an acceptable range of error.

17. Key Words Pavement elastic properties measurement; GPR method, correlation between elastic property and electrical property		18. Distribution Statement No restrictions. This document is available to the public through the National Technical Information Service, Springfield, Virginia 22161 www.ntis.gov.	
19. Security Classif. (of this report) Unclassified	20. Security Classif. (of this page) Unclassified	21. No. of Pages 62	22. Price

Form DOT F 1700.7 (8-72) Reproduction of completed page authorized
This form was electrically by Elite Federal Forms Inc.

Feasibility Study of Non-Contact, High-Speed Elastic Property Measurement of Pavements

by

Aditya Ekbote, Huichun Xing, Jing Li, Xuemin Chen, and Richard Liu

Technical Report 0-4827-2

Project Number: 0-4827
Project title: Feasibility Study of Non-Contact,
High-Speed Elastic Property Measurement of Pavements

by the

Subsurface Sensing Laboratory
Department of Electrical and Computer Engineering
University of Houston

December 2005

DISCLAIMER

The contents of this report reflect the views of the authors, who are responsible for the facts and the accuracy of the data presented herein. The contents do not necessarily reflect the official view or policies of the Federal Highway Administration (FHWA) or the Texas Department of Transportation (TxDOT). This report does not constitute a standard, specification, or regulation.

University of Houston

4800 Calhoun Rd.

Houston, TX 77204

ACKNOWLEDGMENTS

TABLE OF CONTENTS

LIST OF FIGURES

LIST OF TABLES

Chapter 1: Introduction

1.1 Background and Overview

Elastic properties of pavements are important factors in pavement design and maintenance. Traditionally, the pavement elastic properties can be measured by the devices like the Plate Load (PL), the Falling Weight Deflectometer (FWD), and the Rolling Dynamic Deflectometer (RDD).

The PL is a static device used for measuring the elastic properties of pavements. This system measures the vertical movements of a bearing plate that is placed on the pavement surface when loads are applied on and released from the bearing plate in increments. By correlating the quantities of the applied loads and the vertical movements of the bearing plate, the elastic modulus of the pavement can be obtained. The plate load test provides accurate results but is limited in its potential for continuous testing because the device is at rest when the measurements are taken. This is due to the need of stationary loads and having the bearing plates piled up on the material surface.

The FWD is a stop-and-go impulse device. It generates a load pulse by dropping a weight on a damped spring system mounted on a footplate. The weight, the spring system, and the drop height can be adjusted to achieve the desired impact loading on the pavement. The impact is applied to the pavement through a steel disk. The deflections of the pavement surface are measured using geophones at 7 locations near the load. The recorded deflections are used to find the elastic modulus for the pavement layers. The FWD has been used to evaluate the structural capacity of flexible, semi-rigid, and rigid pavements to evaluate the load transfer in joints of concrete pavements and to perform field control of sub grades and aggregate layers of pavement.

The RDD is a commercial-sized truck equipped with a servo-hydraulic vibrator that is capable of applying large monotonic sinusoidal loads to the pavement. However, due to the fact that the displacement sensors are geophones and need physical contact with the materials to be measured, both FWD and RDD vehicles have to be stopped and sensors set up every time measurements have to be made, which makes measurements slow to conduct network level measurements. This also makes it difficult to collect data

1

on an open road. Extreme precaution has to be taken, and traffic control has to be enforced prior to the measurements.

This purpose of this research is to study two aspects: 1) replacing geophone sensors by laser sensors because laser sensors make non-contact measurements and have a very high accuracy in pavement deflection measurements; 2) the relationship between elastic and electrical properties of pavement materials and to find methods to derive elastic property values of pavement materials by measuring their electrical properties because the electrical property measurements can be non-contact, continuous, and at highway speed.

The development and the measured results of the laser sensors for pavement deflection measuring will be discussed in Chapter 2. The electrical property measuring device will be introduced in Chapter 3, and the measured results and correlations with the FWD data will be given in Chapter 4. Conclusions and recommendations are in Chapter 5.

Chapter 2: Measurement of Pavement Deflections Using Falling Weight Deflectometer and Laser Device

2.1 Introduction

Pavement deflections are widely used to compute the elastic modulus of pavements. Traditionally the Falling Weight Deflectometer (FWD) has used geophone sensors for this purpose. In this research, the laser device developed at the University of Houston's Subsurface Sensing Lab was used for measuring the pavement deflections. This research was conducted primarily for flexibility verification of replacing the geophone sensors with the laser device in FWD deflection measurements.

2.2 Falling Weight Deflectometer

The FWD is a stop-and-go impulse device used for measurement of pavement deflections, as shown in Figure 2-1. The deflections of the pavement surface are measured using geophones at seven locations near the load. As seen in Figure 2-1, the loading system of the FWD is attached to a van as a trailer. The loading system consists of a drop beam with different weights that can be attached to or detached from it using the computer inside the van. The weight can be dropped from four available drop heights.

Every time data has to be collected the vehicle is stopped, the load plate and geophones are lowered, and then the weight is dropped several times to record the data.

2.2.1 Geophone Construction and Setup

The geophone consists mainly of two components: a coil and a magnet. The geophone has an outer housing of magnet, and a coil is suspended from a spring on the inner side. The pavement deflects when the load is dropped and so does the outer housing of the geophone, since it is in contact with the pavement. However, due to the fact that the coil is suspended by a damped spring, the coil more or less stays put. This phenomenon

induces a small current into the coil, which represents the velocity of the pavement deflections. This signal is then amplified and processed to give deflection readings.

The geophone is a contact sensor; hence, it is required to be set down on the pavement prior to dropping the load and again picked up before driving the vehicle to next location of interest. TXDOT uses FWD, which has seven such geophones lined up with a separation of 12 inches, as seen in Figure 2-2 [5]. The closest one to the load impact is located at the center of the load plate.

Figure 2-1 Falling weight deflectometer
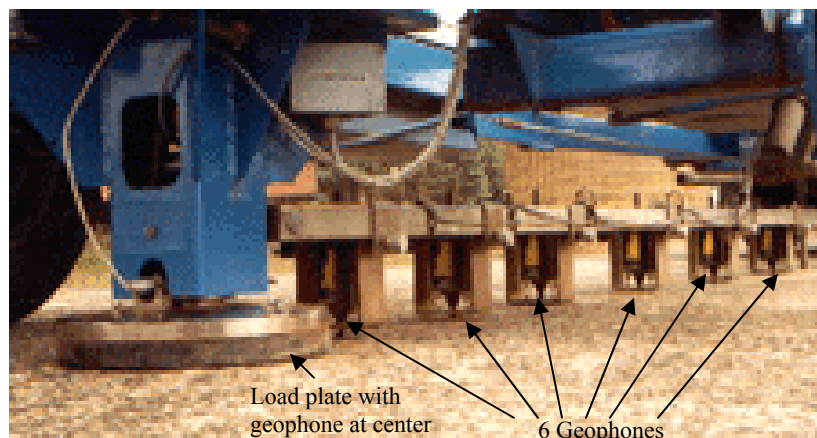
Figure 2-2 Geophone setup on the FWD

2.2.2 Data Collection and Interpretation

The FWD has the capability of storing pavement deflection history from the time the load is dropped onto the pavement for the time interval of 30 ms, as shown in Figure 2-3. For most applications, only the peak deflections measured by each sensor are used for further analysis. For study purposes, it can be observed that sensor D1, located at the center of the load plate, records maximum deflection. The deflections recorded by D1, D2, D3, D4, D5, D6 and D7 decrease sequentially as the sensors are located away from the point of impact.
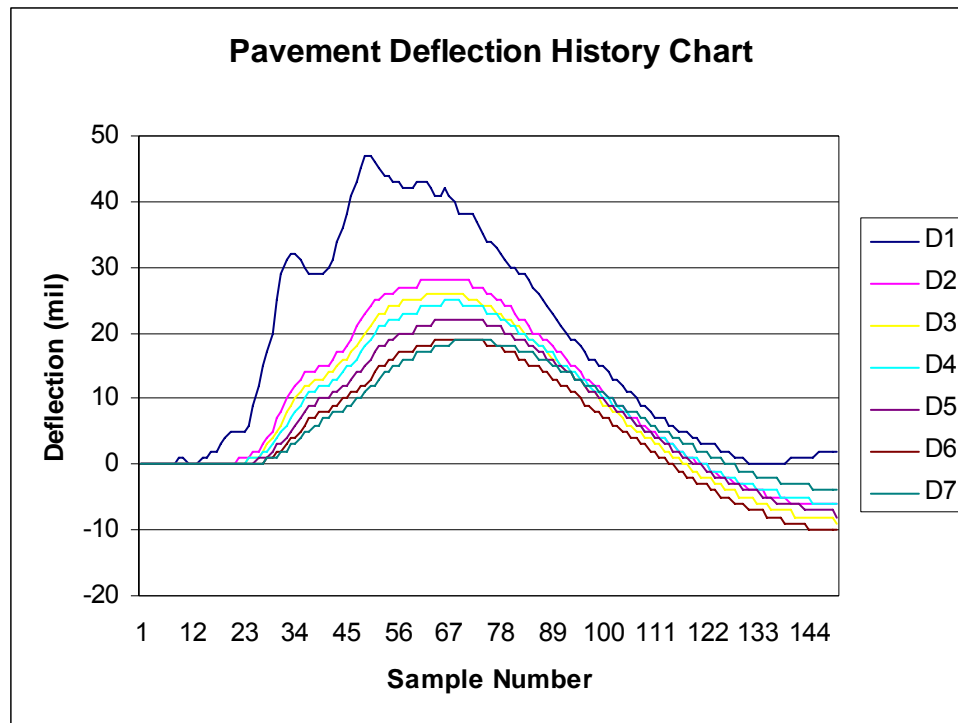
Figure 2-3 Pavement deflection time history chart

The deflection characteristic of the pavement discussed above gives rise to a deflection basin, as shown in Figure 2-4. Previous research has shown that certain parts of the deflection bowl are influenced by the different pavement layers. With reference to Figure 2-4, the chosen criteria are usually geophones d1, d6 and (d1-d4). The central deflection, d1, gives an indication of the overall pavement performance, while the

deflection difference, (d1-d4), relates to the condition of the bound pavement layers. Deflection d6 is an indication of the sub-grade condition [6].
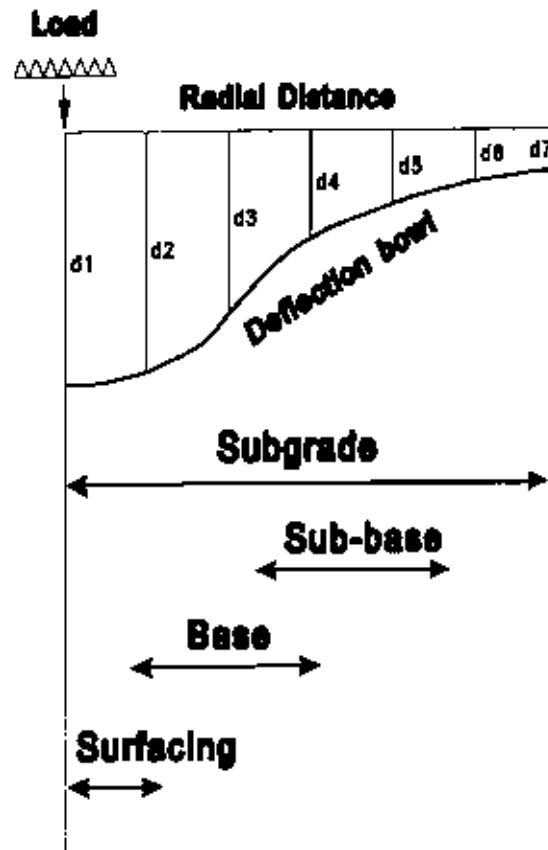
Figure 2-4 FWD deflection bowl

2.3 Measurement of Pavement Deflection Using the Laser Device

2.3.1 Triangular Principle

The laser device used for measurement of pavement deflection works on the triangulation principle [7]. Figure 2-5 demonstrates the geometry of image formation. The laser beam intercepts the optical axis at point A and the reflected laser spot located at point A′ (on the position detector). Image B′ corresponds to point B.

According to the law of image focusing, the following relationships can be expressed as

$$\frac{1}{f} = \frac{1}{L} + \frac{1}{L'} \qquad (3\text{-}1)$$

where f is the focus length of the lens, L is the linear distance between object and focus lens, and L' is the linear distance between the focus lens and position detector.
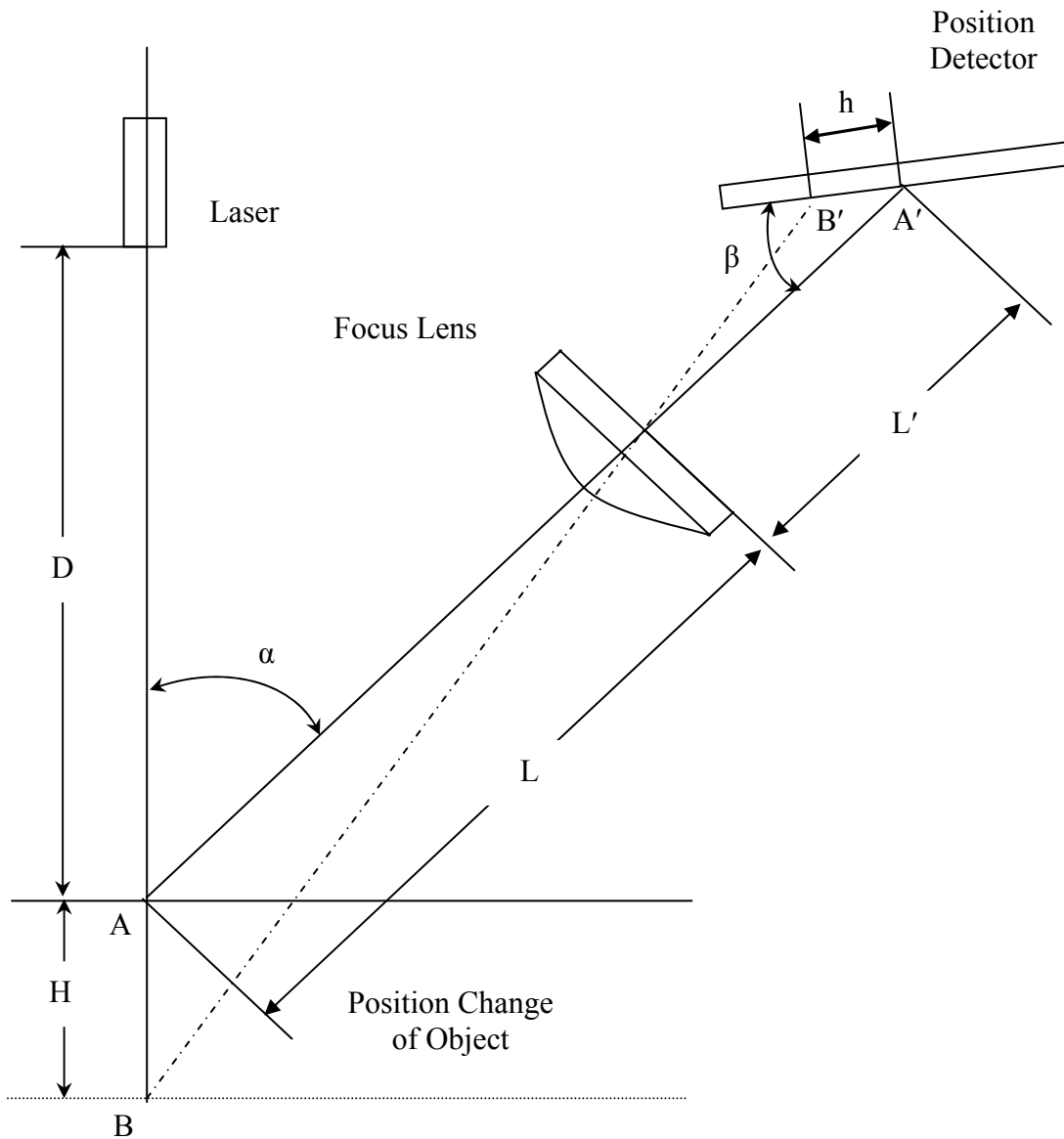
Figure 2-5 Triangulation principle

In Figure 2-5, α is the angle between the projected laser beam and reflected laser beam, and β is the angle of the reflected laser beam on the position detector. The relationship of α and β can be expressed as

$$\tan\beta = \frac{(L-f)}{f}\tan\alpha, \qquad (3\text{-}2)$$

where H is the sensing range, and h is the corresponding position change of the laser spot on the position detector. The change of h can be calculated by

$$h = \frac{Hf\sin\alpha}{(H\sin\alpha - f)\sin\beta}. \qquad (3\text{-}3)$$

2.3.2 Equipment Setup and Experiment Procedure

The laser device was mounted on a push cart and positioned at 20 inches from the center of the loading plate of the FWD, as shown in Figure 2-6. Accelerometers were installed on the push cart and the FWD frame to compute and compensate vibrations of the push cart frame when the weight is dropped by the FWD.

Figure 2-6 Laser device setup

The FWD was used to apply the load on the pavement five times with an average force of 16630 lbf. The pavement deflections were measured using the FWD and the laser device at each drop.

Since the pushcart or the FWD frame, referred to as laser frame, on which the laser device is mounted will vibrate after the falling weight impacts on the pavement, this frame vibration causes errors to the laser-measured deflections. To solve this problem, the accelerometers are employed to measure the vibration of the laser frame. The acceleration data recorded was integrated twice to get the vibrations in mils. Finally, the pavement deflections measured using the laser was compensated for the laser frame vibration using the measured frame vibration. The pavement deflections using the laser device and the FWD were compared.

2.3.3 Results

Figure 2-7 shows the results for pavement deflections obtained using the laser device for the four FWD drops. The Y-Axis represents deflections in mils, and X-Axis represents time in seconds.
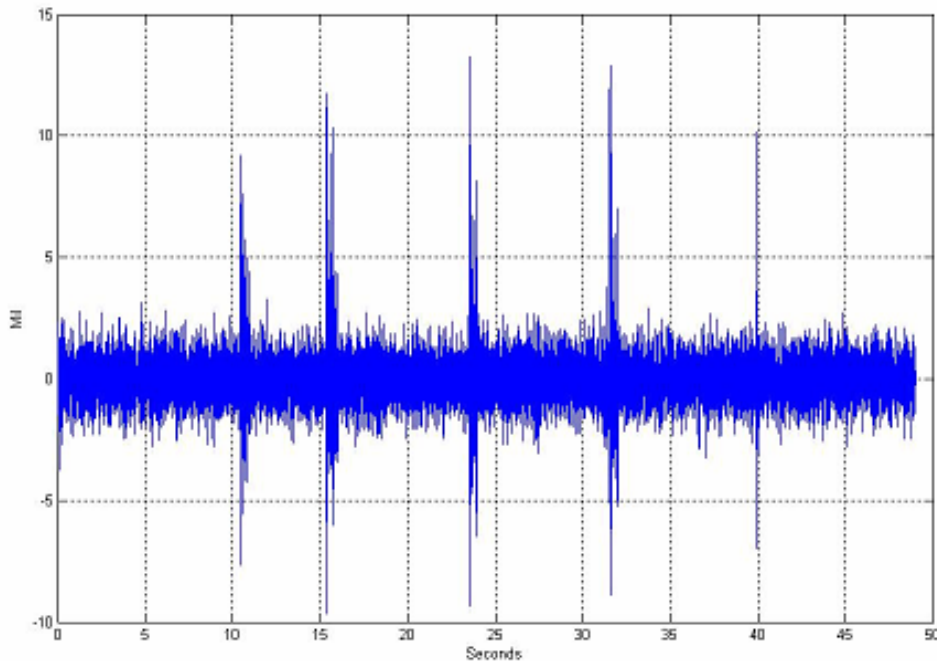
Figure 2-7 Laser results

9

Figure 2-8 shows the laser frame vibrations measured using the accelerometer. The Y-Axis represents the vibrations in mils, and the X-Axis represents the time in seconds.
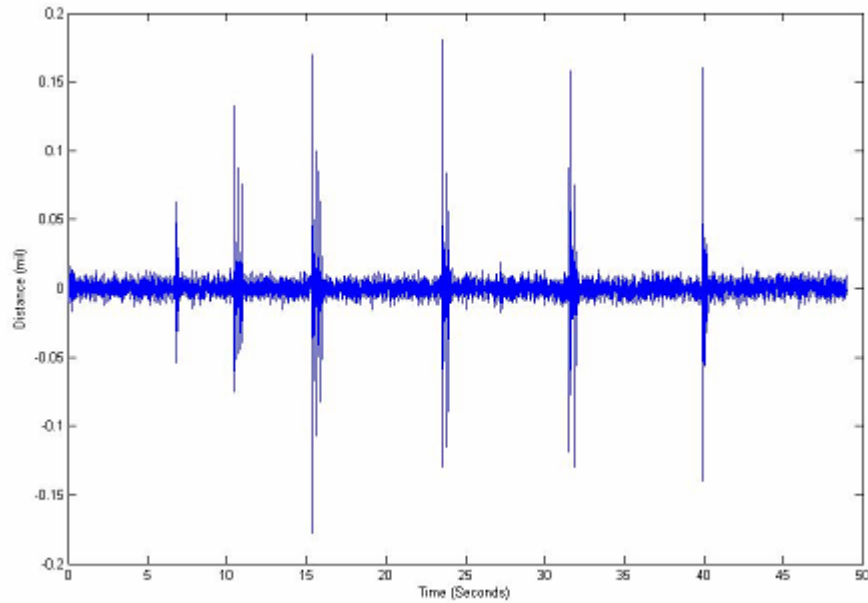
Figure 2-8 Frame vibrations measured by accelerometer

Figure 2-8 shows that six vibrations are recorded. The first vibration in the laser frame is recorded when the loading plate is initially lowered as a part of the FWD setup sequence. The average frame vibration recorded by the accelerometer was 0.15 mils.

After compensating the effect of the laser frame vibration from the recorded deflections, the pavement deflections using the laser device and FWD were compared. Table 2-1 shows the results obtained using the FWD and the laser device for deflections measured at 20 inches from the point of load impact.

Table 2-1 Pavement deflections measured by the laser device and the FWD

	Deflections Using Laser (mils)	Deflections Using FWD (mils)
Drop 1	9.65	12.5
Drop 2	12.17	12.43
Drop 3	13.37	13.05
Drop 4	13.5	13.2
Drop 5	10.15	12.5

The final results verified that the laser device measured results are very close to the results measured by FWD geophone sensors. Laser sensors are verified to be capable of replacing current geophone sensors.

Chapter 3: GPR Device for Measuring Electrical Properties of Pavement

3.1 Introduction

Theoretically, the elastic properties of pavement materials are correlated with their electrical properties. The measurement of elastic properties should be achieved indirectly by measuring electrical properties of the pavement. To accurately measure the electrical properties of pavement, both time-domain and frequency-domain measurement methods were investigated. The Pulse GPR system developed by the Subsurface Sensing Lab, University of Houston, is based on time domain measurement at a lower frequency band. It is modified in this project to measure elastic properties of deep pavement layers. The Frequency Modulated Continuous Wave (FMCW) GPR is used to measure top pavement layers, especially thin asphalt layers, to increase the resolution. The high-frequency and low-frequency devices complement each other to cover all pavement layers.

3.2 Pulse GPR System

The working principle of the Pulse GPR system is very straightforward, referenced in Figure 3-1. When the control unit receives a command from the host computer, it triggers the transmitter to emit a short-pulse wave into space via the transmitting antenna. At the same time, the control unit also sends a command to the sampling unit to pick up the incoming reflected signals. The transmitted wave from the transmitting antenna usually propagates in all directions in space, and part of it penetrates into the pavement. When the penetrated wave encounters the subsurface interface, it is reflected back and picked up by the receiving antenna. There is also another part of the transmitted wave propagating directly from the transmitting antenna to the receiving antenna or from the transmitting antenna to the pavement surface and then bouncing up to the receiving antenna, which is called the direct wave. The received direct wave and subsurface reflected wave are both transferred to the host laptop by sampling unit and

data acquisition card. By processing the received signals like removing rebar's influence [14] and finding coming time of reflected waves [13], the thickness, dielectric constant and moisture content of the pavement can be obtained and displayed [13][16]. Figure 3-2 shows vehicle-mounted version of the Pulse GPR developed at the University of Houston.
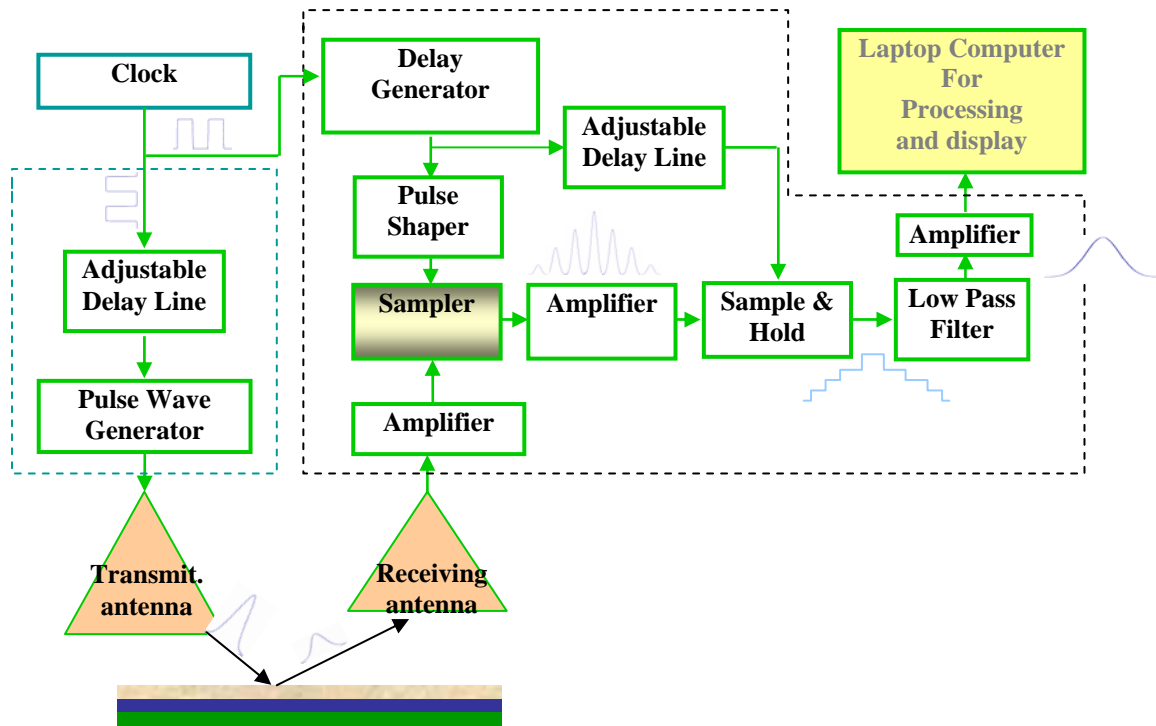
Figure 3-1 Block diagram of the pulse GPR system

Figure 3-2 Pushcart version of the pulse GPR

3.3 Frequency Modulated Continuous Wave (FMCW) GPR

The FMCW GPR is a high-frequency system that is composed of a sweeping transmitter, a receiver, and a computer for data acquisition and system control, as shown in Figure 3-3. It can be seen that this device is a typical frequency modulated continuous wave (FMCW) radar. The lab experimental device using FMCW concept is shown in Figure 3-4. The system can be used to measures the dielectric constant and the conductivity of pavement layers in the frequency range of 3 to 6 GHz. Due to the fact that the dielectric constant, the conductivity, and the elastic modulus of materials are strong functions of the material density, the elastic properties can be obtained by measuring the electrical properties of the pavement material.

A typical FMCW GPR consists of a transmitter sending a microwave signal to the pavement and a receiver receiving the signal reflected back from different pavement layers. The receiver is synchronized with the transmitter. The signal coming back from the pavement is received and processed by the analog and digital circuits. The computer acquires the output of the circuits and processes the data, converting it into electrical

properties of each pavement layer and then correlating the dielectric constant and the conductivity to the elastic values.

Figure 3-3 Block diagram of the FMCW radar
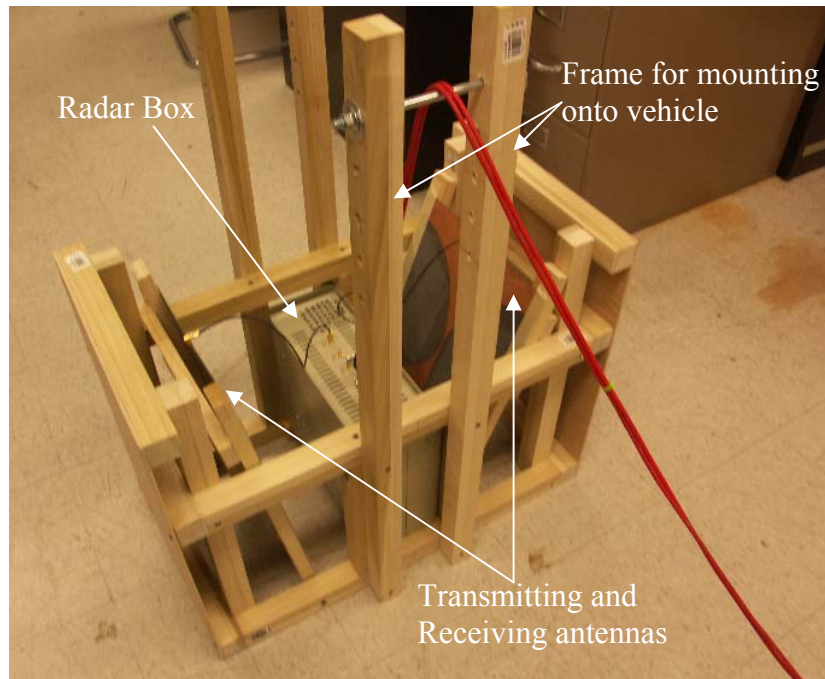
**Figure 3-4 The FM-CW system used for measuring electrical properties
of the pavement layers**

Both the Pulse GPR and the FMCW GPR are non-contact devices that transmit a signal trace and receive the response signal in a few milliseconds. If the vehicle on which the microwave system is mounted travels at a speed of 60 miles per hour, these systems can complete one measurement before the vehicle moves a distance about five inches. However, the penetration depth of the time-domain microwave system is much higher, which makes it the better choice for measuring electrical properties of several pavement layers.

3.4 Data Processing

There are two ways to correlate the measured GPR data with the elastic properties of pavements. The first way includes two major issues: (1) converting measured EM waves into electrical properties of the pavement layers; and (2) converting electrical properties to elastic indicators. The second way is to directly extract certain characteristics of the GPR waveforms that are determined by pavement materials, and then to correlate the extracted characteristics to the elastic properties of pavements.

Before the conversion of GPR data into elastic properties of pavements, the measured GPR data must be preprocessed, including filtering to remove anomalies and using multiple stages of differentiation method [13] for layer information extraction. With the preprocessed data, the characteristic extraction algorithm can be applied to get the pavement-material-related characteristics, and the inversion algorithm can be applied to convert filtered EM data into electrical properties of each layer using the modified layer inversion method [14]. Here, the layer information of the pavement includes the thickness of each layer, electrical properties of each layer, and possible defects (sink holes, air voids, and segregation). Once the electrical properties of the pavement layers have been obtained, the methods developed in the following chapters have to be used to convert the electrical properties to elastic properties.

3.5 Distance Measurement Instrument (DMI) and Global Positioning System (GPS)

The vehicle mounted version of the GPR allowed a faster data production rate, but it also brought out a new challenge in the form of distance measurement. The encoder used on the pushcart was not rugged and fast enough to measure distance/speed of the vehicle traveling at 30 miles/hour or more. Thankfully, the vehicle acquired from the TXDOT has a distance measurement device and a GPS system preinstalled in it. In order to utilize this equipment, further study was done to understand the communication protocol used by them to transfer data to the computer. As shown in Figure 3-5, the DMI/GPS is connected to a data acquisition box. The data acquisition box consists of an I/O module and a biscuit PC with a serial port and one Ethernet port. The data acquisition box is connected to a router, and the computer is also connected to the router. The data acquisition box is programmed so that it broadcasts the incoming data from the DMI or GPS 4 times/second over the Ethernet port. Figure 3-6 shows the equipment setup inside the vehicle.
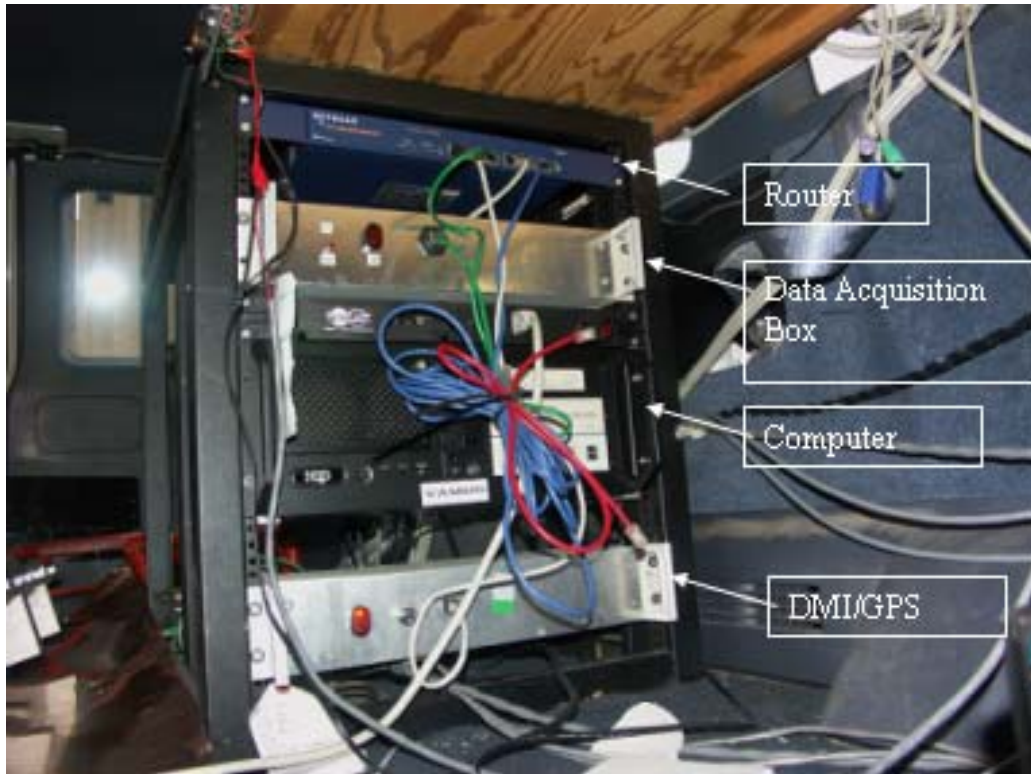
Figure 3-5 DMI and GPS equipment setup

The whole system uses User Datagram Protocol (UDP) for communication. UDP is often referred to as a connectionless network protocol because it does not form a continuous link between the server and the client. The data is broadcast in the form of a fixed size datagram or packets. This ensures faster data transfer but is also error prone, since often data packets are received out of order or are lost. However, in order to comply with the protocol used by the TXDOT vehicle, UDP was used for communication.

```
            ┌─────────────────┐
            │    DMI/GPS      │
            └─────────────────┘
                     │
                     ▼
        ┌──────────────────────┐
        │  Data Acquisition Box │
        └──────────────────────┘
                     │
                     ▼
        ┌──────────────────────┐              ╭────────────╮
        │    Ethernet Port     │              │   RJ 45    │
        └──────────────────────┘              │  Ethernet  │
                     ▲                        │   links    │
                     │                        ╰────────────╯
        ┌──────────────────────┐
        │       Router         │
        └──────────────────────┘              ┌──────────────┐
                     ▲                         │   Computer   │
                     └─────────────────────────└──────────────┘
```
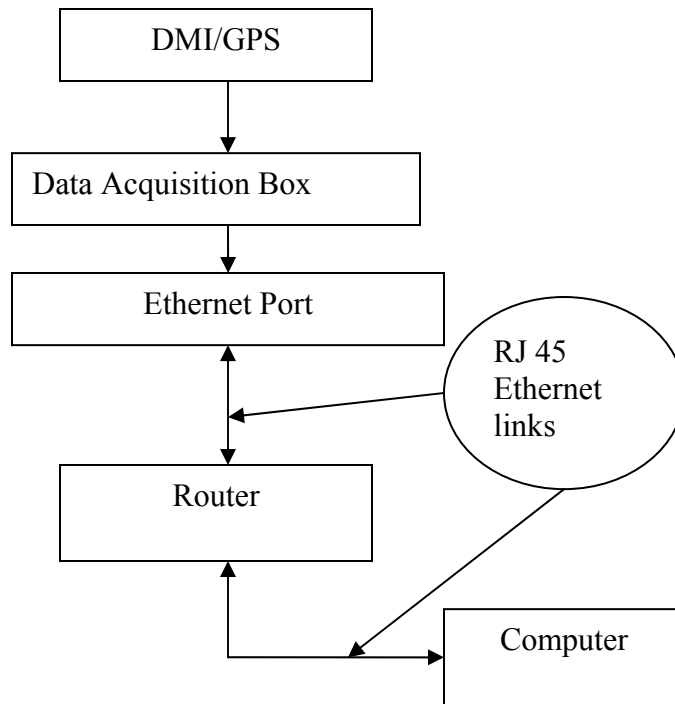
Figure 3-6 DMI/GPS setup

Integrating DMI and GPS data into measured pavement property data would be a great help for the future study and pavement history observation.

Chapter 4: Correlation Between the Elastic and Electrical Properties of Pavement Materials

4.1 Introduction

A step-by-step approach was used to corroborate the proposed methods for measurement of pavement deflections using ground penetrating radar. Initially, simple lab experiments were performed to confirm the relationship between the density of asphalt and its dielectric constant. These experiments were followed by field tests on test pads using the GPR and the FWD. The FWD and the GPR data was then processed and compared. The relationship between the two data sets was mapped and curve fitted to give an empirical relationship between the deflection of pavements and the processed GPR data. As the final step, GPR data was collected from a section of pavement at an interval of 5 feet, and the calculated pavement deflection results were compared with the data collected using FWD.

4.2 Relationship Between the Density and Dielectric Constant of Materials

The objective of this experiment was to confirm the relationship between the density of asphalt slab and its dielectric constant. One of the asphalt slabs was constructed using 960 pounds of asphalt, which was poured into a wooden box that was 30.75 Inch wide and 64 Inch long, as shown in Figure 4-1 and Figure 4-2.

Figure 4-1 Asphalt slabs for lab experiment

Data wascollected several times at different densities using both Frequency Modulated Continuous Wave Radar and Pulse GPR.
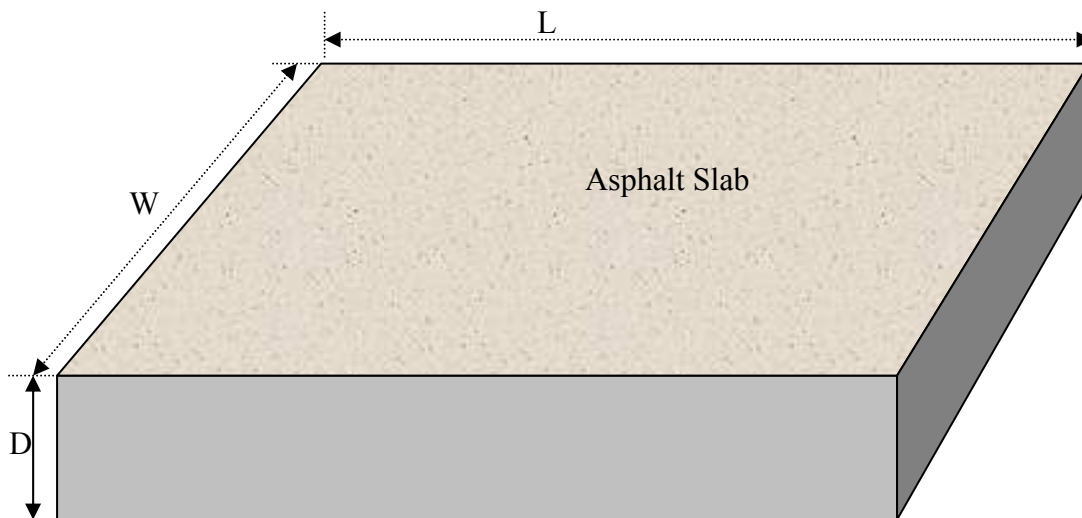
Figure 4-2 Asphalt slab in the lab, where L = 64 Inch and W = 30.75 Inch

Once the slab was constructed, the initial density was 0.0424 pound/inch^3, and the height of the slab was 11.5 Inch. This was followed by measurement of the dielectric constant of the slab using both the Frequency Modulating Continuous Wave (FM-CW) GPR and Pulse GPR. This collection of steps was called Test 1. A similar procedure was repeated for two more densities by uniformly pressing the asphalt. For Test 2, the height of the slab pressed to 11 Inch; hence, the density of slab was 0.0443 pound/inch^3. Finally for Test 3 the height of the slab was 10.75 Inch and density 0.0453 pound/inch^3.

4.2.1 Test 1 Results

Test 1 was carried out with 0.0424 pound/inch^3 density of the slab. Figure 4-3 and Figure 4-4 show the results obtained with the FM-CW GPR and Pulse GPR, respectively.
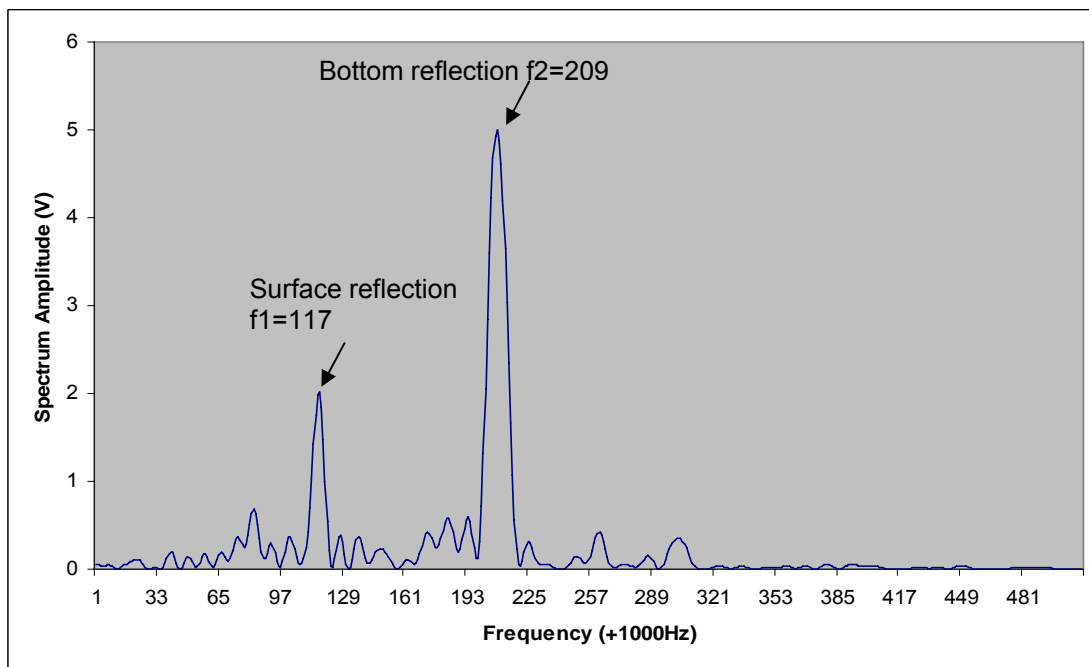
Figure 4-3 Test 1 using the FMCW radar, slab thickness 11.5 Inch

The dielectric constant of the pavement can be estimated from above FMCW radar data as [13]

$$\varepsilon_r^{FM-CW} = (0.04764*(f2-f1)/2*30/2.54/11.5)^2$$
$$= 5.065689 \tag{4-1}$$
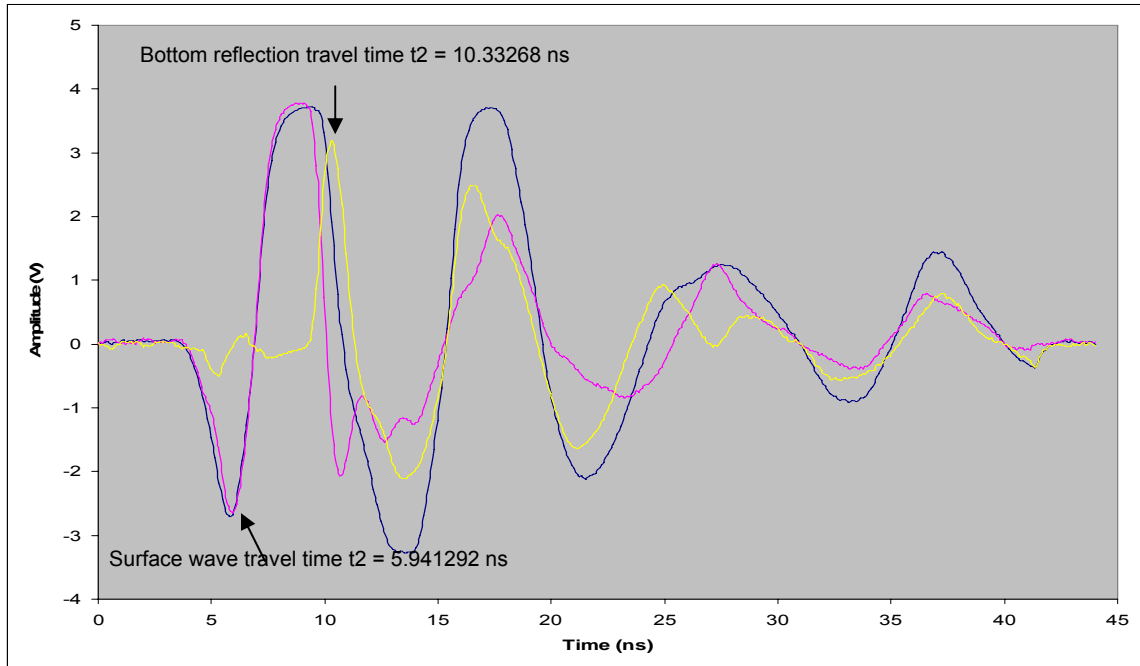
Figure 4-4 Test 1 using the pulse GPR, slab thickness 11.5 Inch

From the pulse GPR data, as shown in Figure 4-4, the dielectric constant can be calculated by

$$\varepsilon_r^{PulseGPR} = ((t2-t1)/2*30/2.54/11.5)^2$$
$$= 5.085375 \tag{4-2}$$

24

4.2.2 Test 2 Results

Test 2 was carried out with 0.0443 pound/inch^3 density of the slab. Figure 4-5 and Figure 4-6 show the results obtained with the FM-CW GPR and Pulse GPR, respectively.
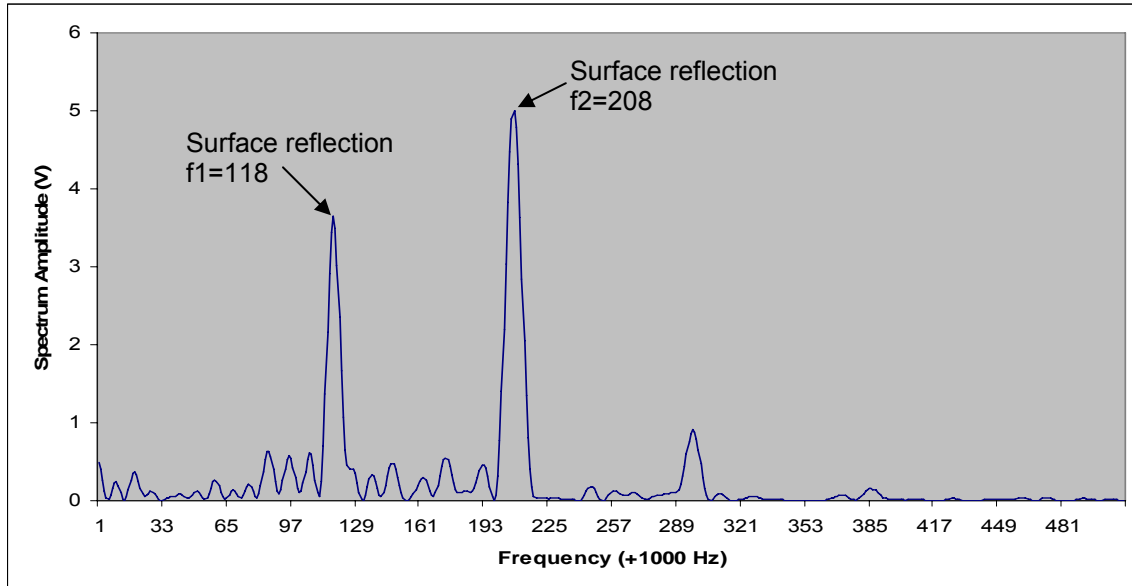
Figure 4-5 Test 2 of the FMCW radar, slab thickness being pressed to 11 Inch

The dielectric constant can be calculated by

$$\varepsilon_r^{\text{FM-CW}} = (0.04764*(f2-f1)/2*30/2.54/11)^2$$
$$= 5.298565 \tag{4-3}$$
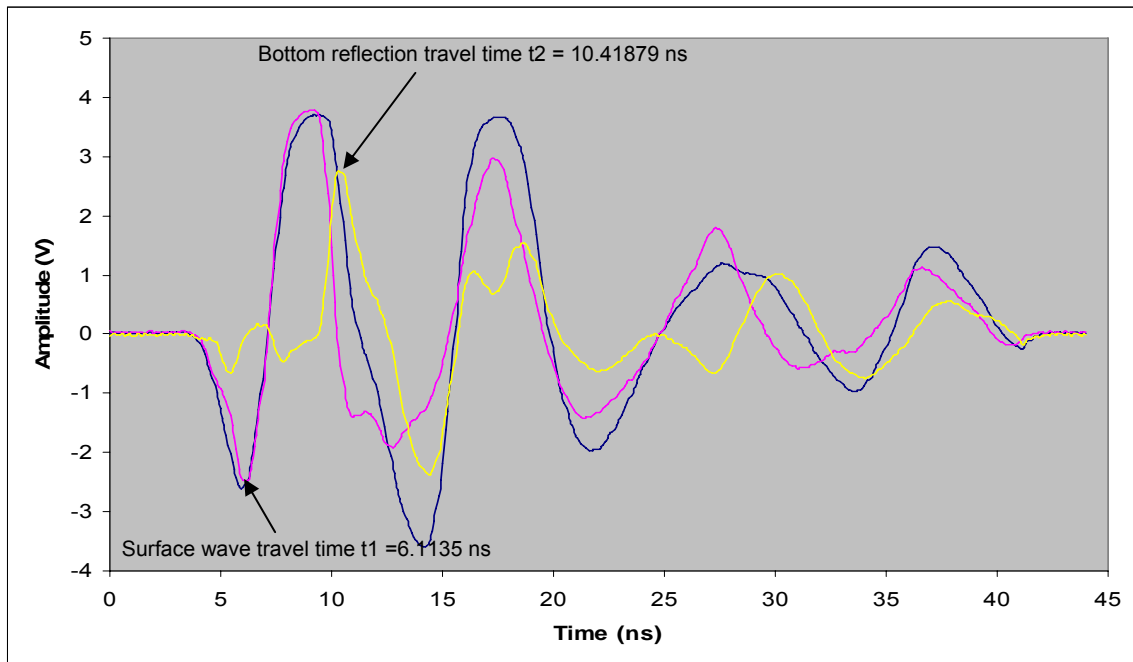
Figure 4-6 Test 2 of the pulse GPR, slab thickness being pressed to 11 Inch

The dielectric constant is

$$\varepsilon_r^{Pulse} = ((t2-t1)/2*30/2.54/11.5)^2$$
$$= 5.342377 \tag{4-4}$$

4.2.3 Test 3 Results

Test 3 was carried out with 0.0453 pound/inch^3 density of the slab. Figure 4-7 and Figure 4-8 show the results obtained with the FM-CW GPR and Pulse GPR, respectively.
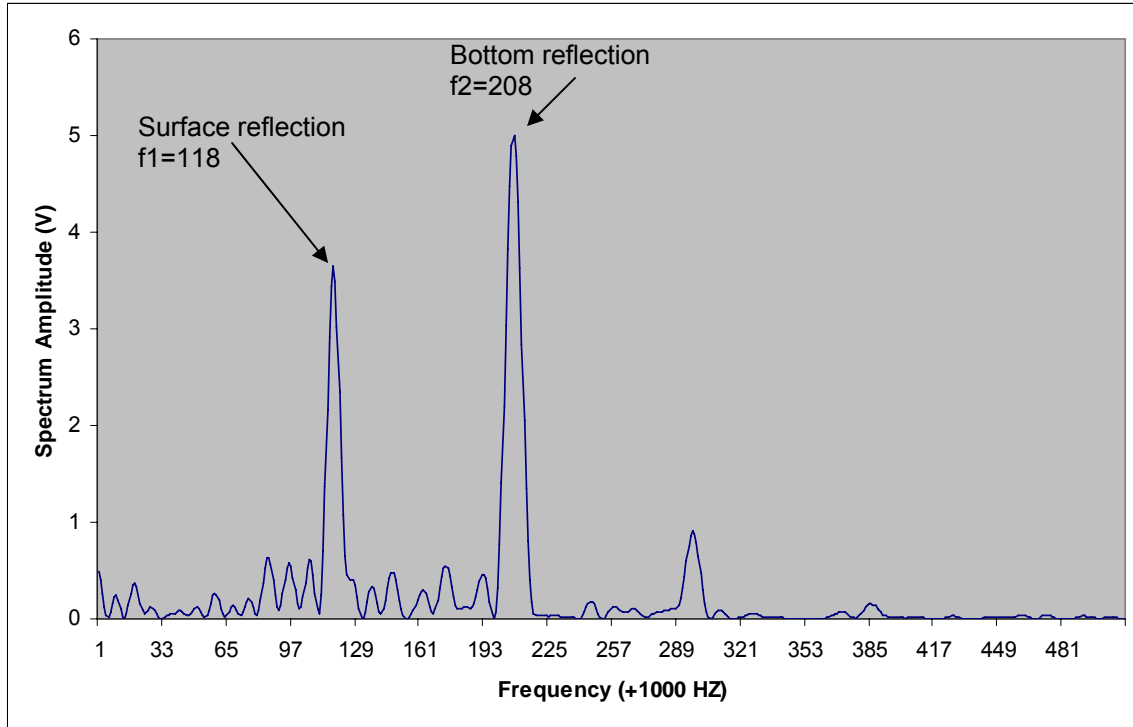
Figure 4-7 Test 3 of the FMCW radar, slab thickness being pressed to 10.75 Inch

The dielectric constant is

$$\varepsilon_r^{FM-CW} = (0.04764*(f2-f1)/2*30/2.54/10.75)^2$$
$$= 5.547875 \tag{4-5}$$
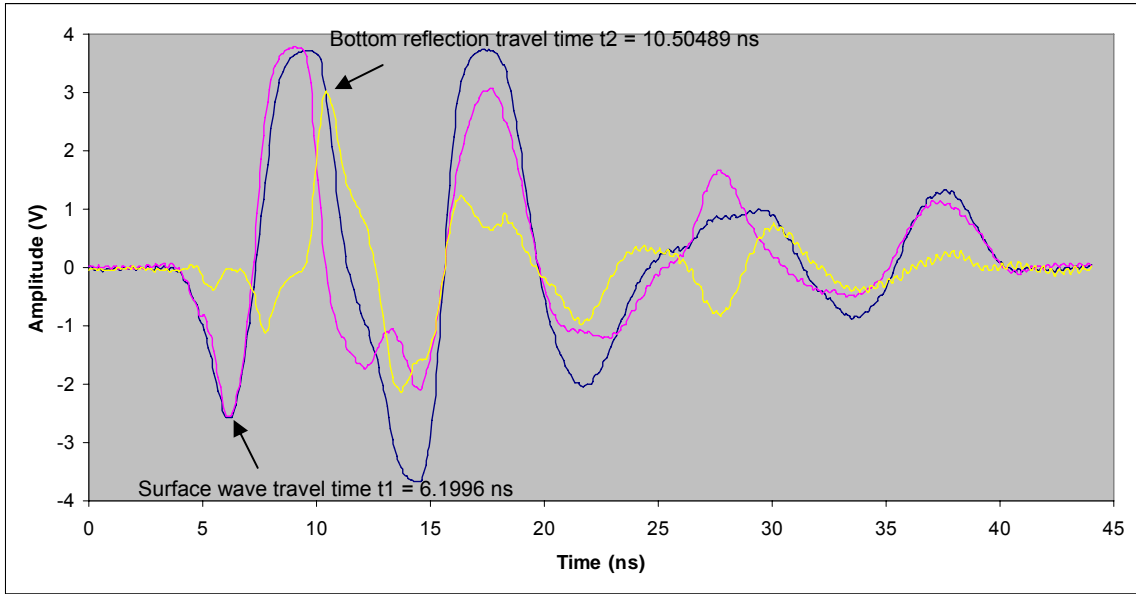
Figure 4-8 Test 3 of the pulse GPR, slab thickness being pressed to 10.75 Inch

The dielectric constant is

$$\varepsilon_r^{Pulse} = ((t2\text{-}t1)/2*30/2.54/10.75)^2$$
$$= 5.593749 \tag{4-6}$$

4.2.4 Lab Test Data Analysis

After completing all the tests, Equation 4-1 through Equation 4-6 give the dielectric constant of the slab measured by FM-CW radar and pulse GPR at different densities. The dielectric constant calculated was plotted against density, as shown in Figure 4-9.

Figure 4-9 evidently shows that the dielectric constant of the asphalt is correlated with its density. The correlation is more of a monotonic correspondence. In order to further investigate the correlation between the pavement deflections and the GPR data field, tests were performed, as discussed in the following chapters.
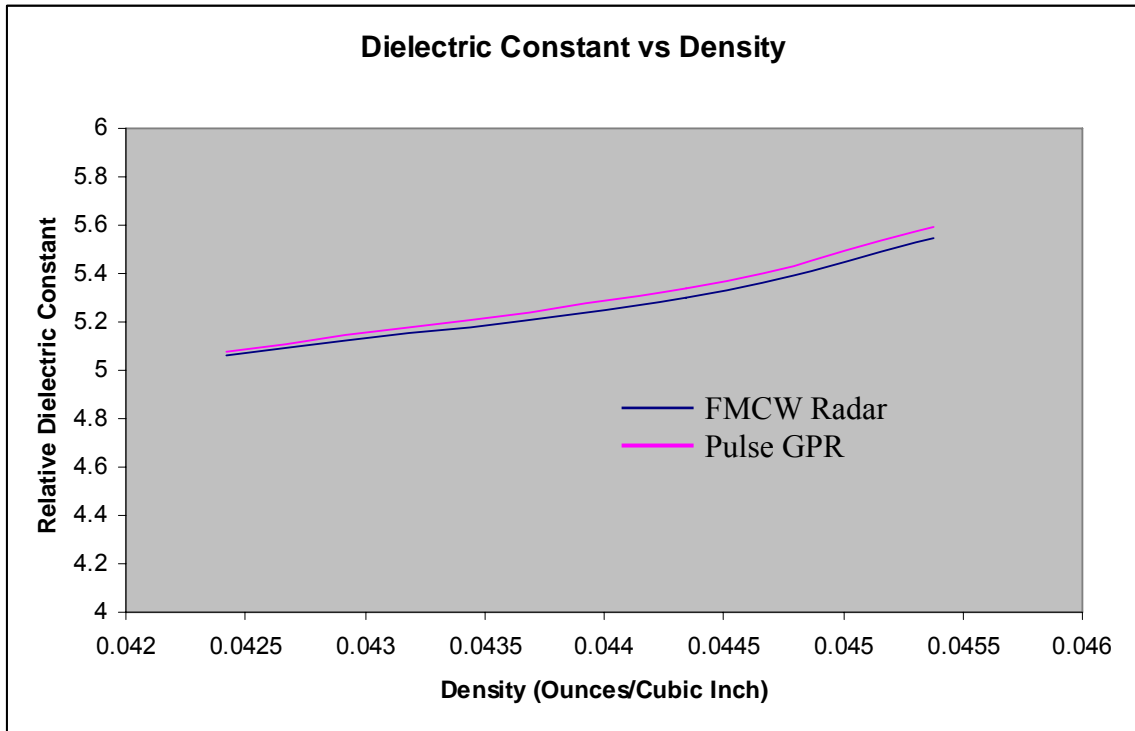
Figure 4-9 Relation between the dielectric constant and density of asphalt material

4.3 Field Tests

All the field tests were performed using the Pulse GPR because of the obvious advantage of the pulse GPR for deeper ground penetration. Henceforth, the Pulse GPR shall be referred to only as GPR.

A series of field tests were performed using GPR and the FWD on several pavement sections. The results obtained using both methods were processed and compared to find an empirical correlation between GPR data and pavement deflections using the FWD.

Four known pavement sections with different Elastic modulus were selected for performing the tests. First, on each section, several GPR traces were collected and stored. The GPR data collection was immediately followed by the FWD data collection. This procedure was followed to ensure similar temperature and moisture content conditions.

4.3.1 Tests at Pad 1
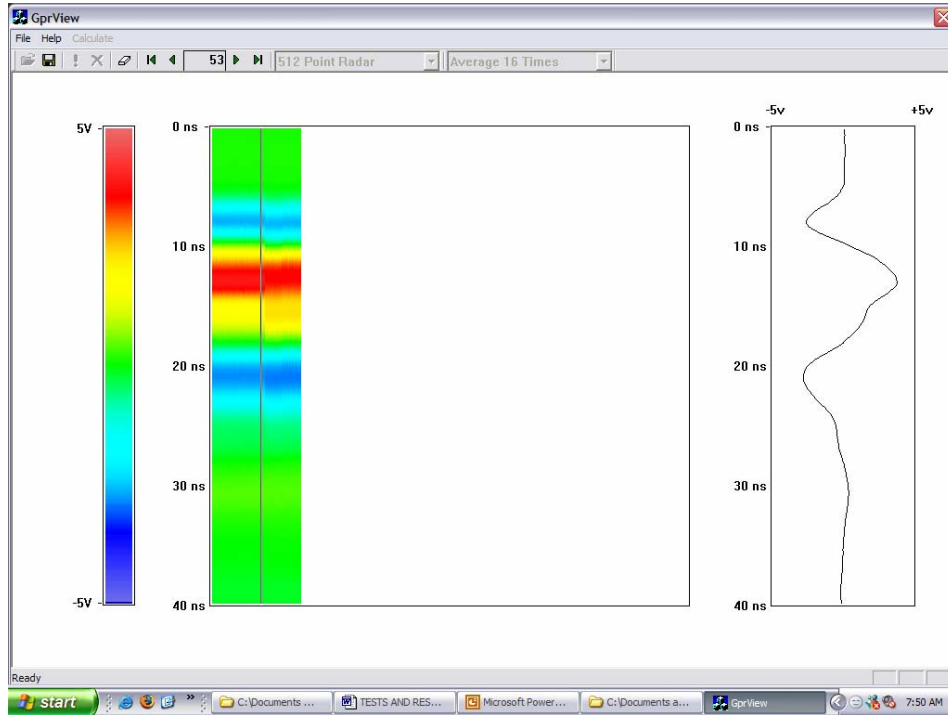
Figure 4-10 GPR trace color-map obtained at pad 1
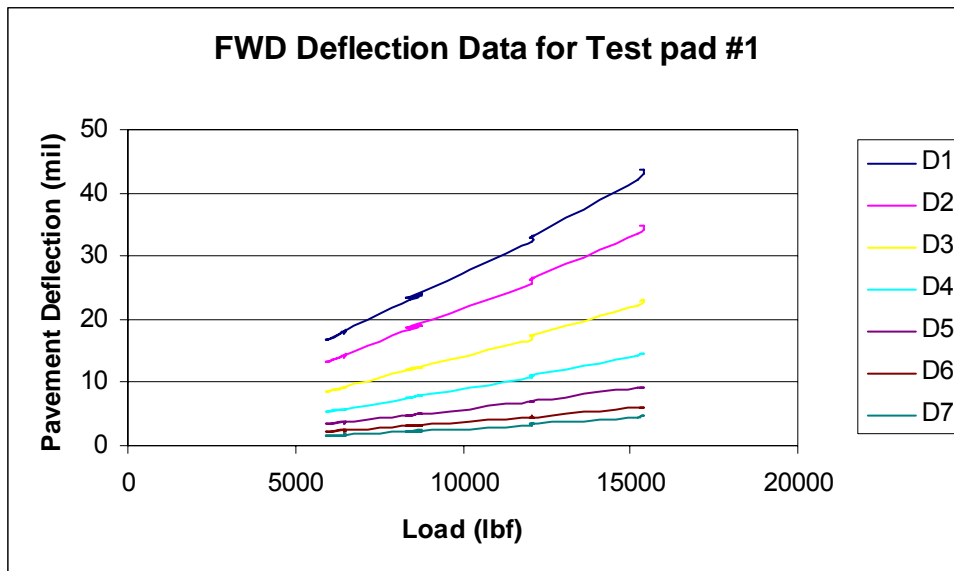
Figure 4-11 Pavement deflection data obtained with the FWD at pad 1

4.3.2 Tests at Pad 2
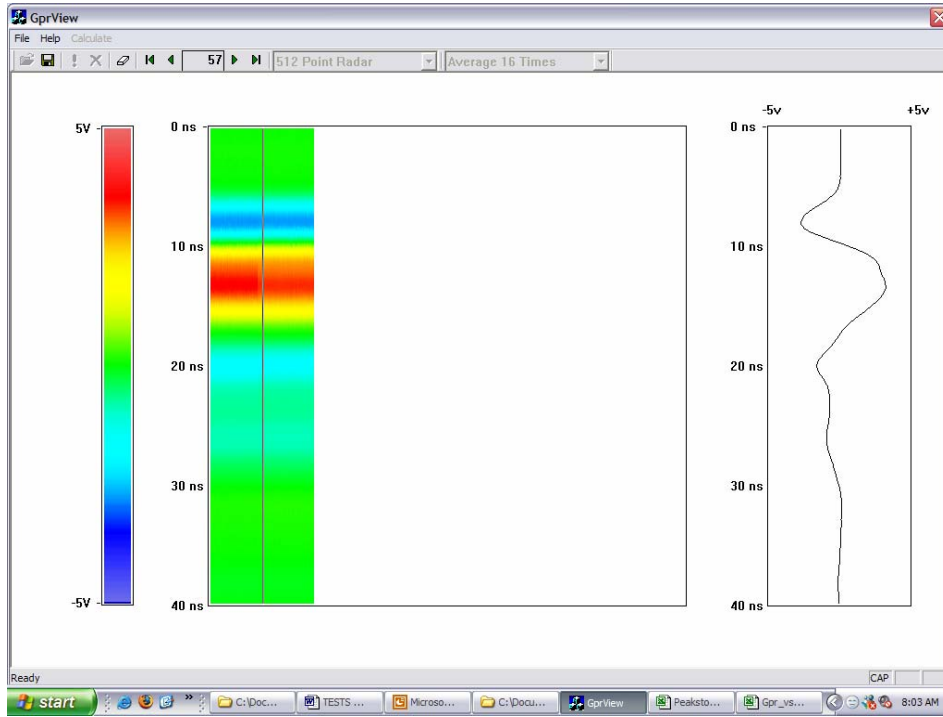
Figure 4-12 GPR trace color-map obtained at pad 2
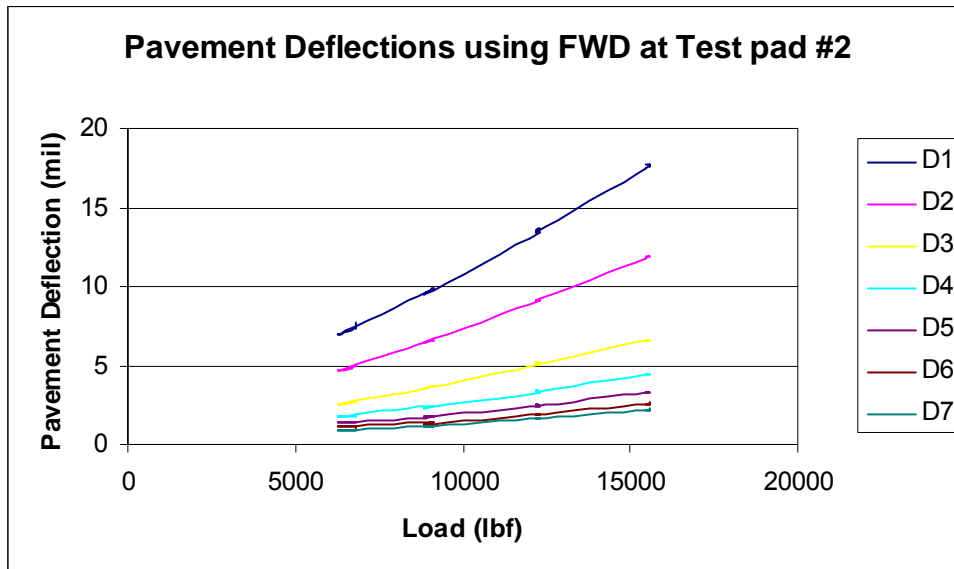
Figure 4-13 Pavement deflection data obtained with the FWD at pad 2

4.3.3 Tests at Pad 3
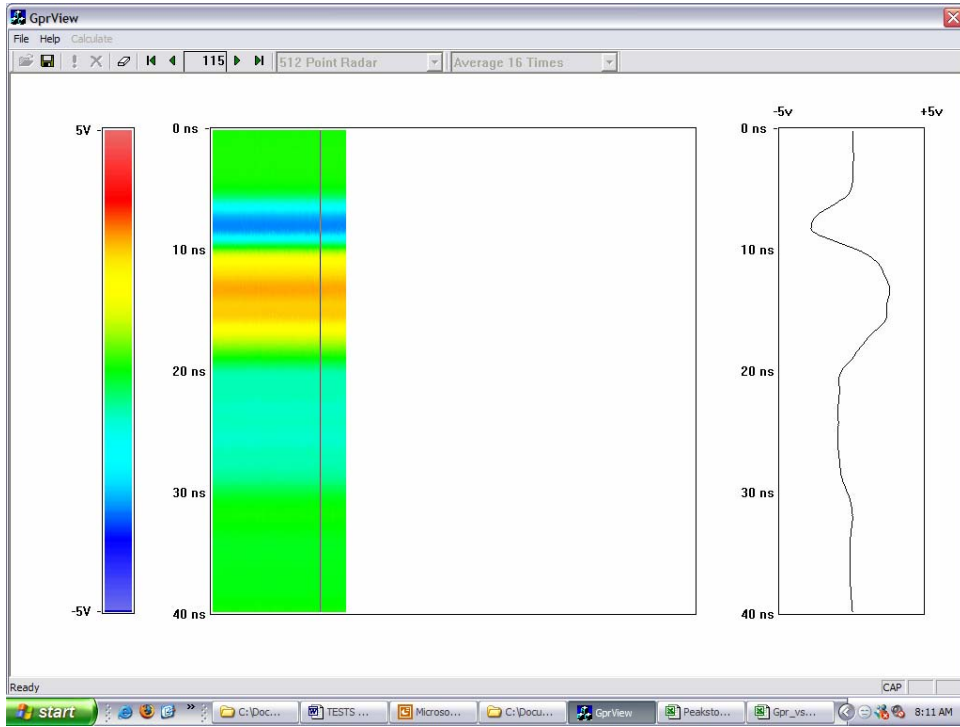
Figure 4-14 GPR trace color-map obtained at pad 3
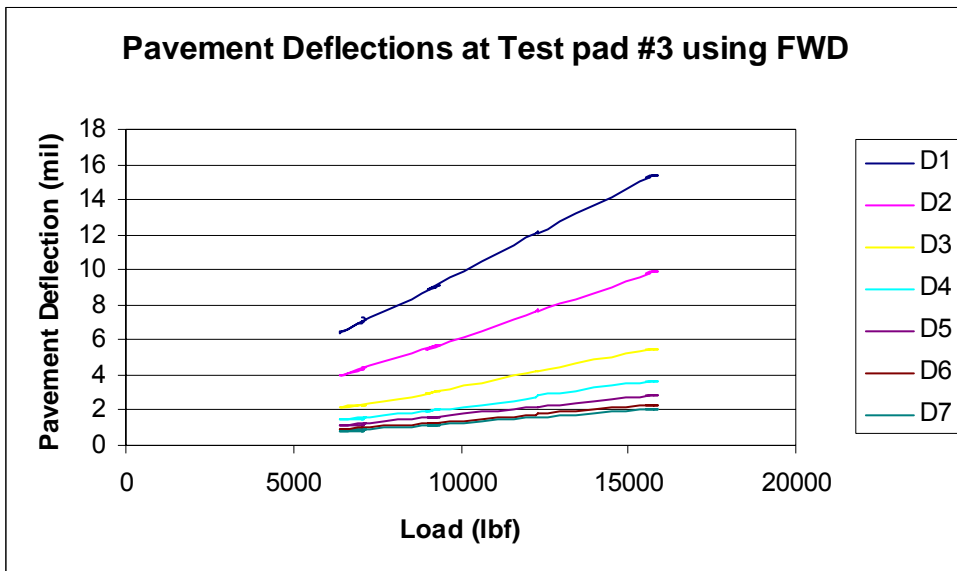
Figure 4-15 Pavement deflection data obtained with the FWD at pad 3

4.3.4 Tests at Pad 4
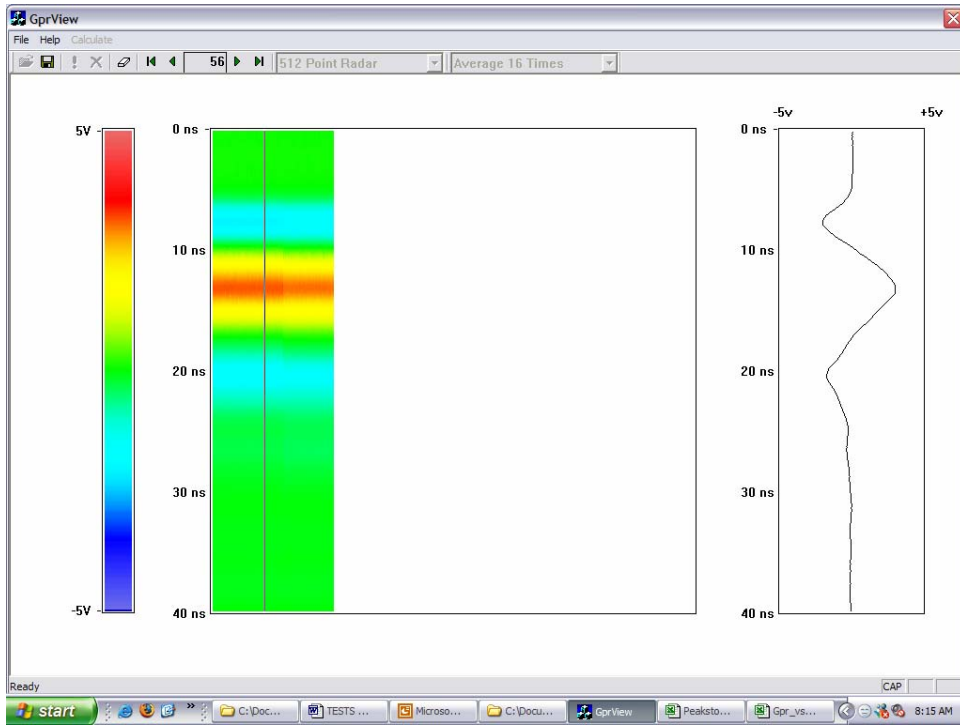
Figure 4-16 GPR trace color-map obtained at pad 4
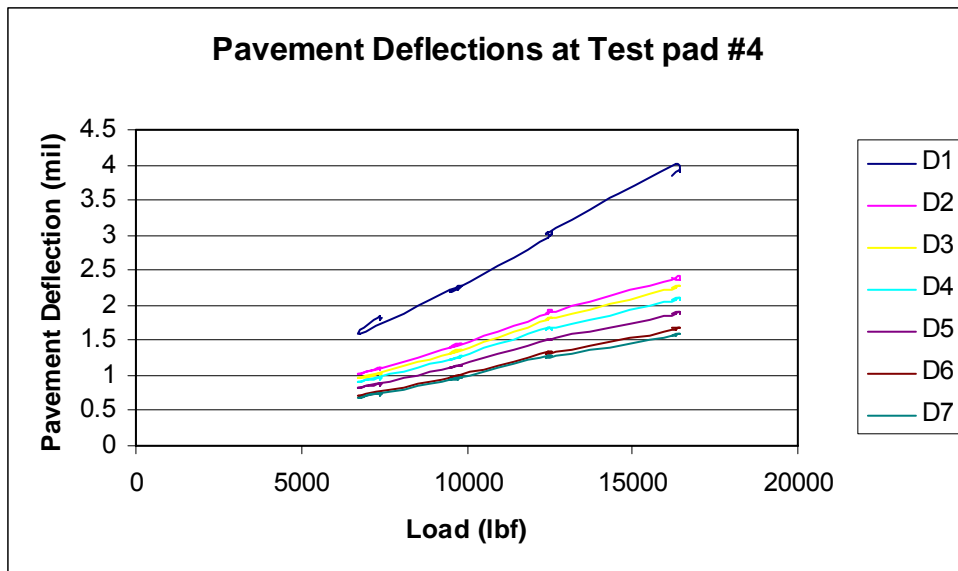
Figure 4-17 Pavement deflection data obtained with the FWD at pad 4

4.3.5 Data Processing

As discussed in the previous chapter, the travel time of the layer reflections is found to be a function of the dielectric constant of pavement materials. However, in our experiments, we found that the DC offset of the GPR traces is not just related to the dielectric constant of the pavement material, but also the conductivity. Hence, it is more reliable to the DC offset as an indicator of GPR measurements. Initially, the GPR traces obtained at each test pad were averaged in order to minimize the influence of any anomalous GPR traces on the final results. Figure 4-18 shows the average traces for all the four pads.
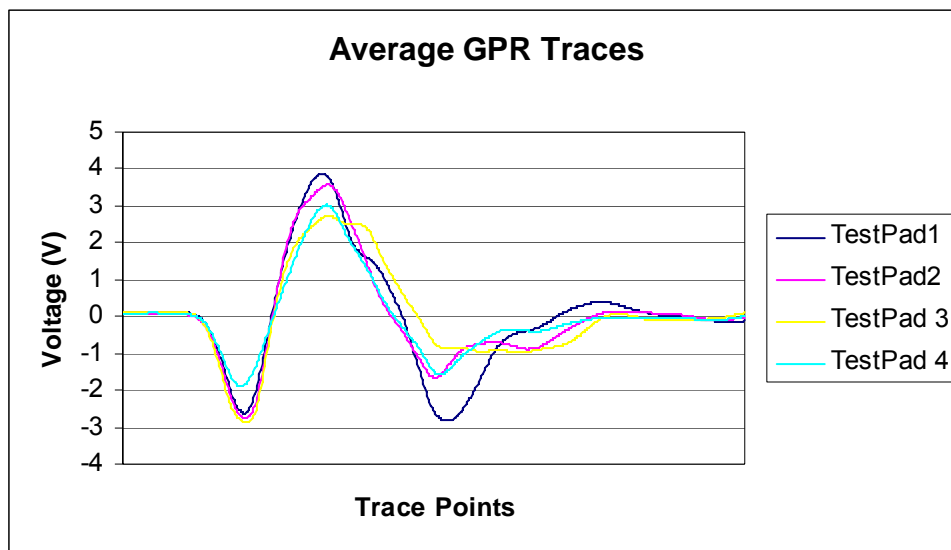
Figure 4-18 Average GPR traces for all test pads

Then, in order to compute the DC offset voltage of the GPR trace, the voltage data at each point of the trace was summed and divided by the number of points in each trace. Table 4-1 shows the GPR DC offset values in voltage along with the FWD data collected for all the seven geophone sensors in mils.

Table 4-1 GPR and FWD collected from four separate test pads

	Pad 1	Pad 2	Pad 3	Pad 4
GPR Trace DC Offset (V)	0.231095	0.087995	0.043123	-0.0589
D7 (mils)	4.56	2.19	2.03	1.58
D6 (mils)	5.98	2.56	2.3	1.67
D5 (mils)	9.16	3.23	2.85	1.89
D4 (mils)	14.6	4.4	3.68	2.08
D3 (mils)	22.91	6.61	5.45	2.25
D2 (mils)	34.72	11.87	9.85	2.39
D1 (mils)	43.55	17.66	15.29	3.85

In order to find the correlation between the GPR data and FWD data, all the data was normalized and plotted together. Table 4-2 shows the normalized data for the GPR and FWD sensors.

Table 4-2 Normalized GPR and FWD sensor data

	Pad 1	Pad 2	Pad 3	Pad 4
GPR Trace DC Offset	1	0.380774	0.186603	-0.25489
D7	1	0.480263	0.445175	0.346491
D6	1	0.428094	0.384615	0.279264
D5	1	0.35262	0.311135	0.206332
D4	1	0.30137	0.252055	0.142466
D3	1	0.28852	0.237887	0.09821
D2	1	0.341878	0.283698	0.068836
D1	1	0.405511	0.351091	0.088404

After finding the DC offset of each averaged GPR trace, the results were normalized. They were then plotted with normalized deflection results recorded for all four test pads, as shown in Figure 4-19.
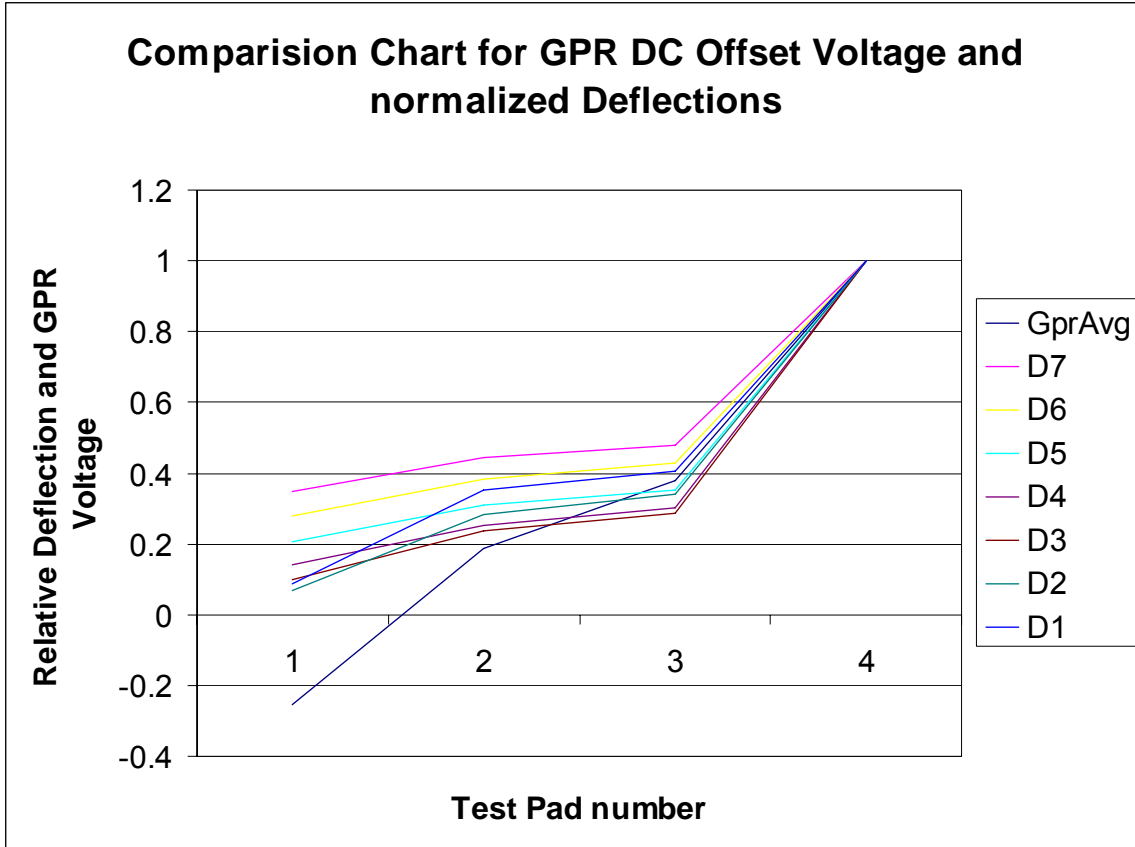
Figure 4-19 Correlation between GPR data and FWD data

4.3.6 Summary of Field Test Results

The field tests concluded that the pavement deflections have a monotonic correspondence with the GPR data. Also, deflections recorded by geophone D1 appear to be relatively in closer correlation with the GPR data compared to the other sensors.

4.4 Measurement of Pavement Deflection Using Pulse Ground Penetrating Radar

4.4.1 Introduction

In order to measure the pavement deflections using ground penetrating radar, the empirical relationship found in the previous chapter was utilized to convert GPR results into normalized pavement deflections.

Initially, a section of pavement was selected for the final tests. Fortunately, the pavement was relatively new and, hence, structurally more stable. The section selected was 0.34 miles long. GPR data was collected at every 0.01 miles, discarding a few readings at the beginning and end of the section. This was done primarily to ensure that the FWD data could be collected later at the exact point. In order to ensure accuracy of a distance interval of 0.01 miles between readings, the DMI was utilized.

After collecting the GPR data, the correlation between the GPR and the FWD found in the previous chapter was used to convert the GPR data into the normalized pavement deflections.

Finally, the FWD was used to measure pavement deflection on the section selected at the same points where the GPR data was collected. The normalized pavement deflections using both methods were compared and analyzed.

4.4.2 GPR Results

One of the GPR data acquired from the pavement section is shown in Figure 4-20.
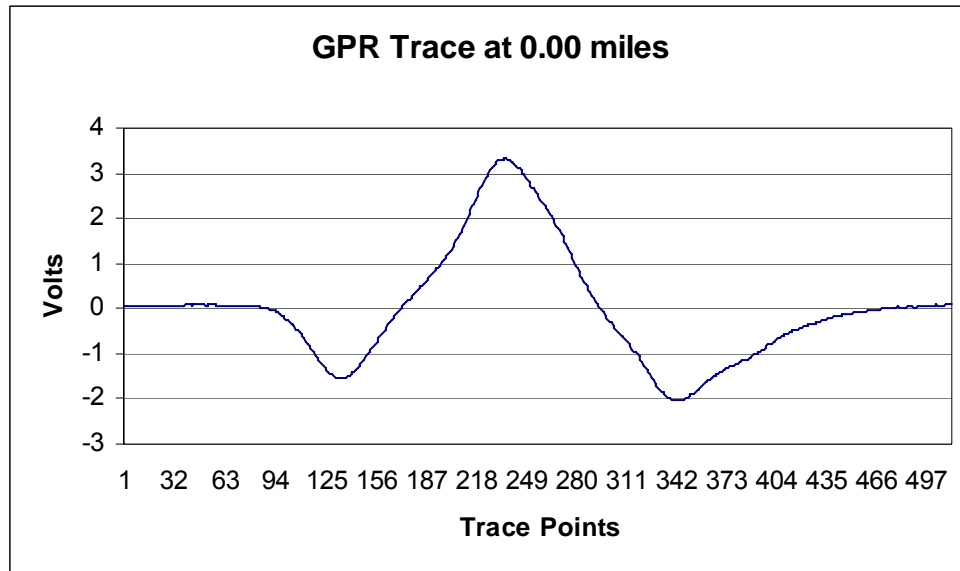
Figure 4-20 GPR trace acquired at 0.00 miles

As mentioned previously, DC Offset voltage was considered as an indication of GPR measurements. Figure 4-21 shows a 3D profile of the GPR data acquired, where the x-axis represents number of traces acquired, y-axis represents GPR voltage in volts, and the z-axis is the number of trace points in each trace.
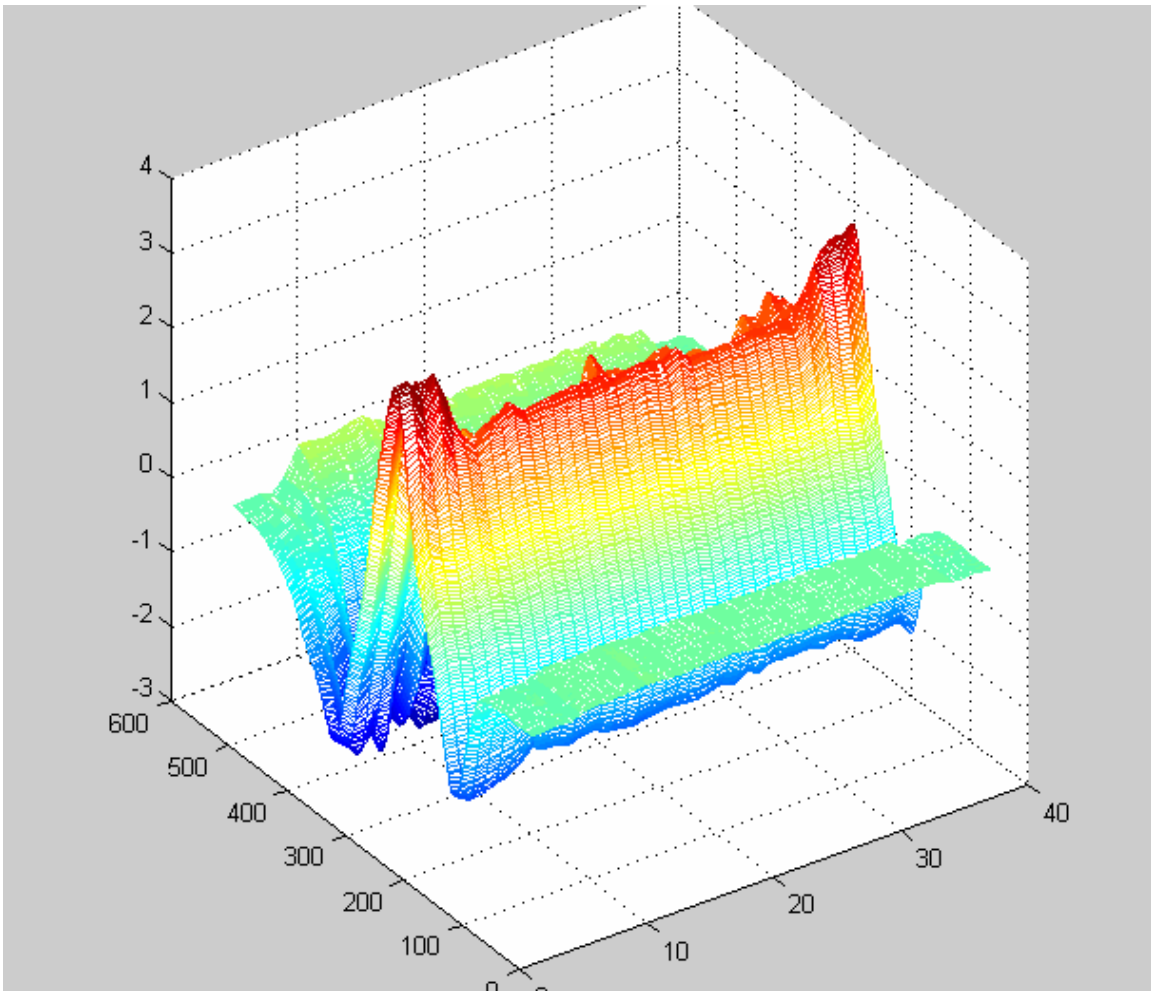
Figure 4-21 3D profile of the GPR data

After collection of the data, for each trace, all the points were averaged in order to find out the DC Offset of the trace. Figure 4-22 shows the profile of the DC offset voltage of all the traces over the pavement section.
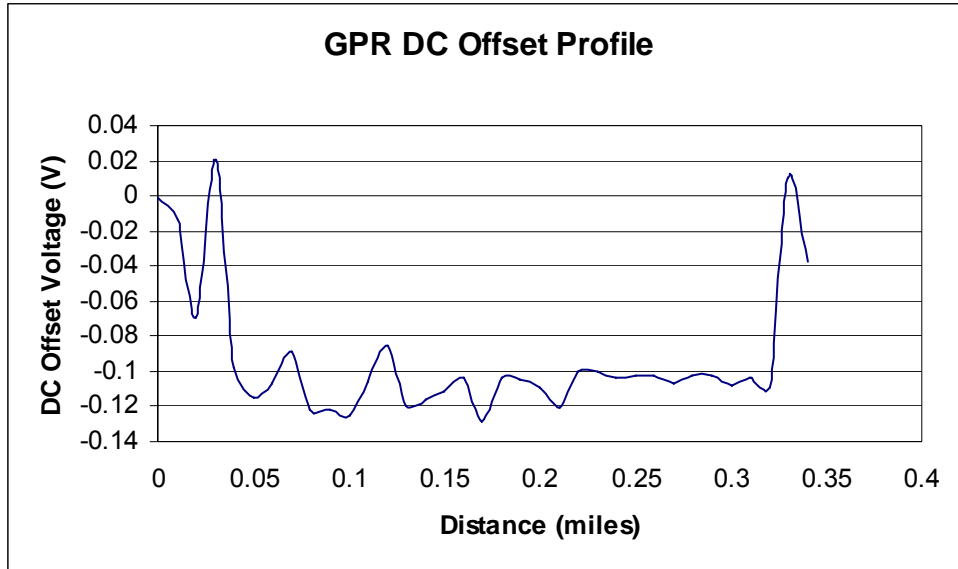
Figure 4-22 GPR DC offset profile

4.4.3 Data Processing

As discussed before, a few measured points were removed from the beginning and the end of the profile, and the rest of the data was normalized. Figure 4-23 shows the profile of the normalized data.
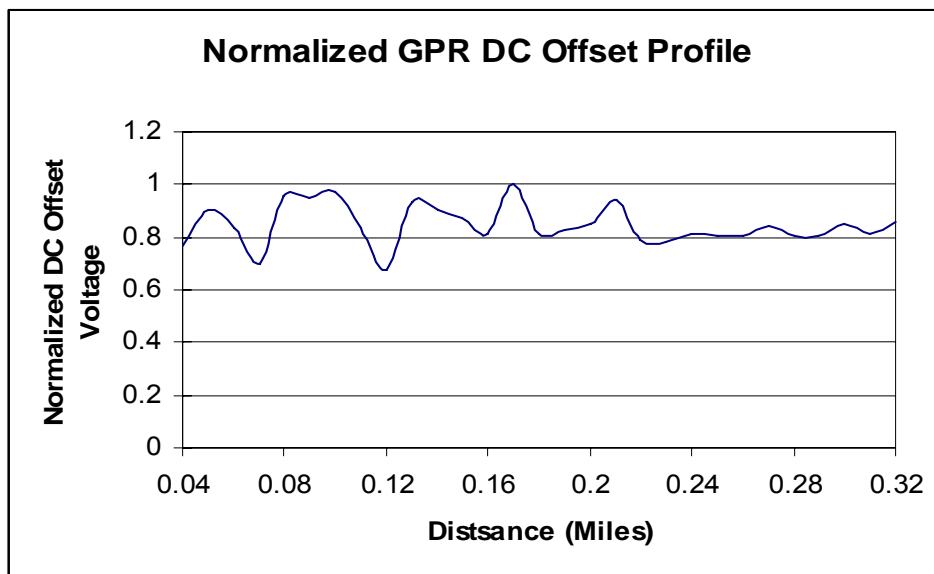
Figure 4-23 Normalized GPR DC offset profile

The normalized GPR data was mapped linearly using the correlation between the GPR data and the FWD found in section 4.3.5. The mapping was performed to get normalized pavement deflections from the GPR data. The following equations were used for the linear mapping:

$$Y = 0.953*X + 0.046 \qquad (4-7)$$
$$Y = 0.300*X + 0.294 \qquad (4-8)$$
$$Y = 0.595*X + 0.462 \qquad (4-9)$$

where Y is the estimated pavement deflection, and X is the measured GPR data.

Equation 4-7 was used when normalized GPR data was greater than 0.38, Equation 4-8 was used when normalized GPR data was greater than 0.186 but less than 0.38, and Equation 4-9 was used when GPR data was less than 0.186.

The equations mentioned above were used to calculate the normalized pavement deflections using the GPR data collected. Figure 4-24 shows the profile of the calculated pavement deflections using GPR.
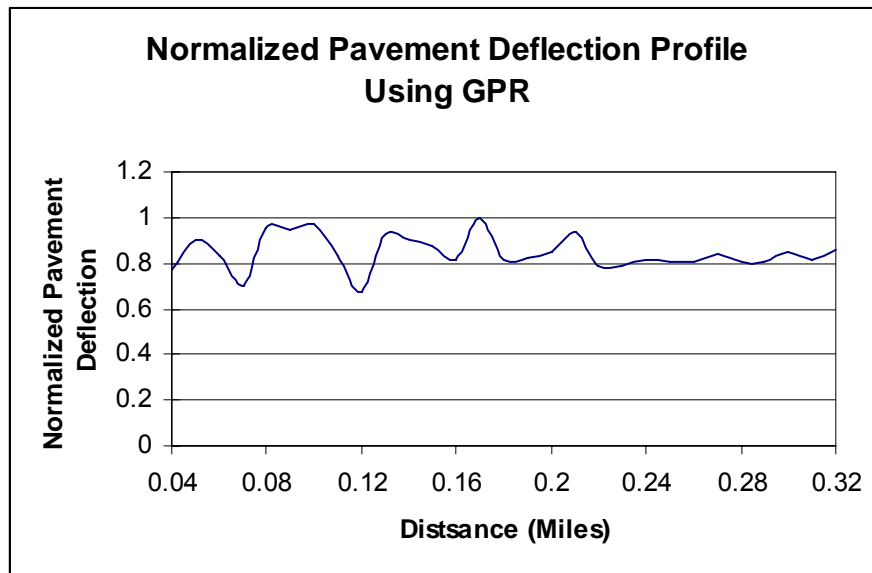
Figure 4-24 Pavement deflections calculated using GPR

4.5 Measurement of Pavement Deflection Using Falling Weight Deflectometer

The FWD was employed to measure pavement deflections physically over the same pavement section. The DMI and GPS system, also installed on the FWD vehicle, ensured precise distance and position of measurement points. Table 4-3 shows the measured pavement deflections.

Table 4-3 Pavement deflections using falling weight deflectometer

Distance (miles)	LOAD (lbf)	D1 (mils)	D2 (mils)	D3 (mils)	D4 (mils)	D5 (mils)	D6 (mils)	D7 (mils)
0	18186	22.76	13.84	9.25	7.09	5.44	4.24	3.46
0.01	18317	23.34	13.58	8.75	6.7	5.1	3.95	3.24
0.02	18063	21.98	13.2	8.62	6.55	4.89	3.69	3
0.03	17928	24.5	14	9.2	7.09	5.32	4.1	3.37
0.04	18250	19.5	11.41	7.31	5.77	4.61	3.8	2.99
0.05	18011	19.56	11.07	7.39	5.87	4.43	3.42	2.88
0.06	17976	19.51	11.43	7.4	5.79	4.52	3.52	2.94
0.07	17749	28.63	17.56	9.93	7	5.15	3.99	3.34
0.08	18007	24.24	11.42	5.7	4.65	3.77	3.09	2.65
0.09	18007	15.9	8.06	5.13	4.33	3.54	2.84	2.39
0.1	17884	18	10.09	6.89	5.56	4.46	3.71	3.29
0.11	17876	16.81	9.82	6.34	4.95	3.87	3.05	2.56
0.12	17769	21.72	12.7	6.89	5.02	3.82	3.03	2.58
0.13	18019	17.28	9.88	6.56	5.09	3.89	3.02	2.46
0.14	17868	21.04	12.27	7.45	5.39	3.98	3.1	2.6
0.15	17729	25.46	14.24	7.95	5.5	3.97	3.04	2.56
0.16	17853	18.95	11.16	6.71	4.98	3.71	2.8	2.28
0.17	17916	17.54	9.68	5.82	4.34	3.25	2.48	2.03
0.18	17666	21.93	12.97	7.67	5.41	3.85	2.89	2.36
0.19	17793	19.59	11.02	6.67	4.76	3.58	2.8	2.31
0.2	17527	24.69	14.26	8.56	5.78	4.28	3.26	2.65
0.21	17817	22.96	13.62	8.54	6.19	4.62	3.59	2.91
0.22	17634	27.03	15.69	9.76	7.15	5.28	3.92	3.11
0.23	17785	22.76	12.45	7.95	5.92	4.3	3.24	2.63

Table 4-3 Pavement deflections using falling weight deflectometer *(continued)*

Distance (miles)	LOAD (lbf)	D1 (mils)	D2 (mils)	D3 (mils)	D4 (mils)	D5 (mils)	D6 (mils)	D7 (mils)
0.24	17646	23.89	13.19	8.59	6.52	4.7	3.6	2.98
0.25	17551	27.02	14.86	9.18	6.67	4.77	3.53	2.84
0.26	17797	18.84	10.1	6.75	5.53	4.36	3.35	2.68
0.27	17721	21.98	13	8.78	6.93	5.34	4.09	3.2
0.28	17841	20.54	11.24	7.02	5.65	4.12	3.08	2.66
0.29	17412	27.81	16.52	10.17	7.43	5.29	3.84	3.04
0.3	17523	27.18	14.81	8.54	6.24	4.62	3.52	2.78
0.31	17416	26.79	14.94	9.58	7.34	5.41	3.89	2.97
0.32	17535	23.74	12.84	7.17	5.01	3.63	2.76	2.28
0.33	17666	20.38	10.72	6.66	5.04	3.78	2.84	2.31
0.34	17308	35.48	19.7	9.41	5.83	3.81	2.87	2.38
0.35	17138	36.46	21.34	10.34	6.36	4.21	3.09	2.64
0.36	17078	43.93	21.36	10.66	7.26	4.89	3.51	2.85

The pavement deflections measured for geophone D1 were normalized and plotted, as shown in Figure 4-25.
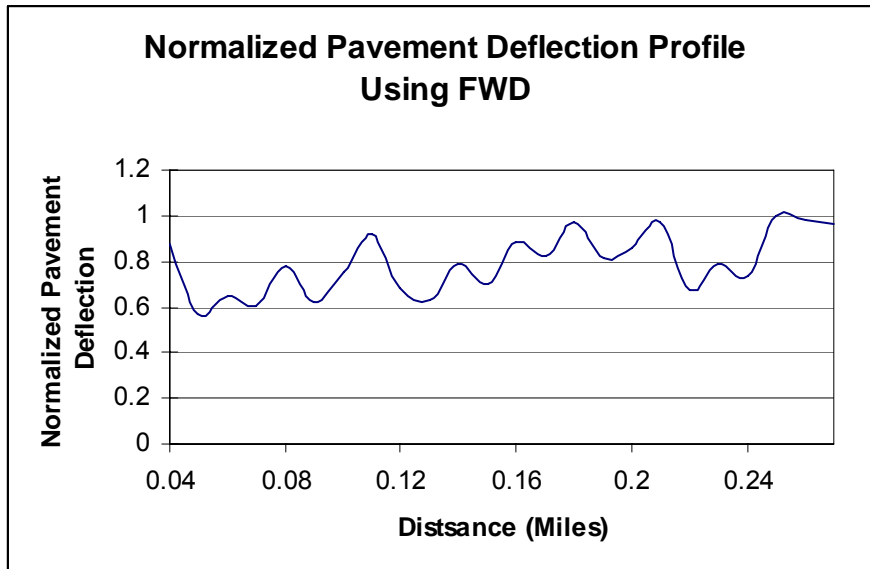
Figure 4-25 Normalized pavement deflections using FWD

4.6 Comparison between Pavement Deflections Measured Using FWD and GPR

The results obtained using both methods were compared with each other. Figure 4-26 shows the profile of the deflections measured using the GPR and FWD.
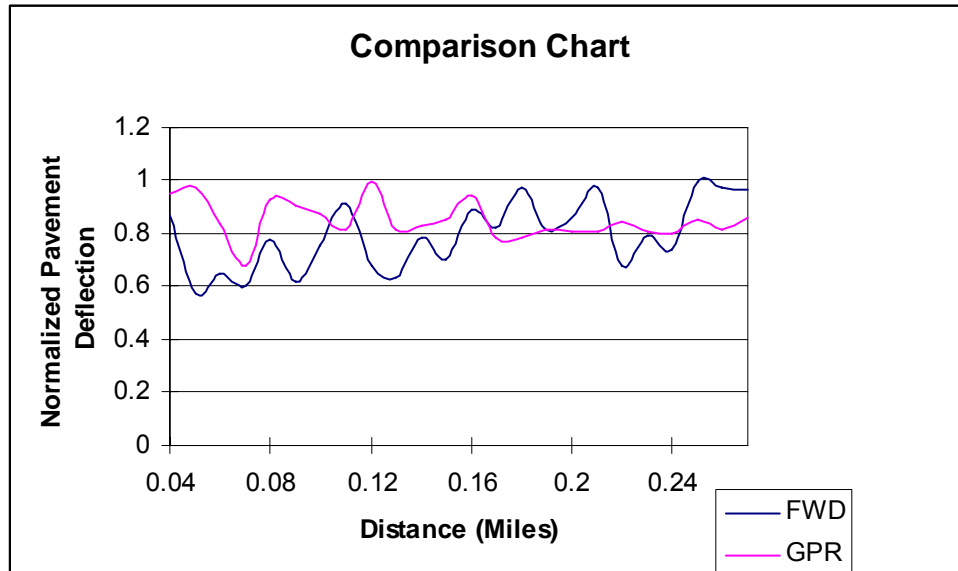
Figure 4-26 Comparison between results obtained using the GPR and FWD

The relative error between the measurements using FWD and GPR was under the acceptable range. For 80% of the measurements, the relative error was below 0.2. Figure 4-27 shows a column chart with the measurements and relative error for each measurement.
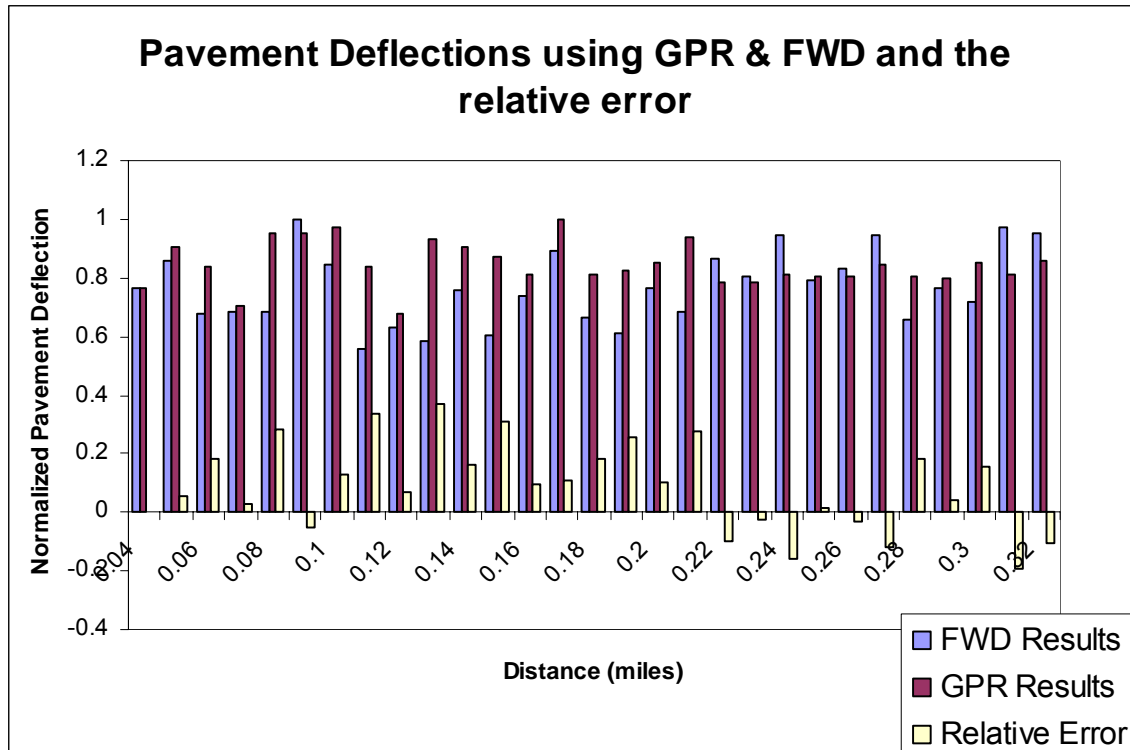
Figure 4-27 Pavement deflection results with relative error

The results obtained using the GPR agreed with the FWD results to a large extent. This confirmed that a correlation exists between the electrical and elastic properties of pavement materials. However, to correctly estimate pavement deflections using the GPR, it is required that we use a correlation obtained from a similar kind of pavement structure. This shows that presently the GPR can be used as a device for the preliminary determination of non-homogenous characteristics in the pavement sections. If the pavement sections are found to be non-homogenous, further tests can be performed using the FWD. This procedure will reduce much time and effort when measuring elastic characteristics on longer pavement sections of a few miles or more.

Chapter 5: Conclusions and Recommendations

The goal of this research was to find a high-speed, non-contact method to measure the elastic properties of pavement materials such as the GPR. In order to achieve this, two methods have been investigated. The first one is the laser sensor method that is used to replace geophone sensors in measuring deflections of pavements. With the compensation of the accelerometer data of the laser frame, the measured deflections by laser sensors have been verified to be very accurate. The second one is GPR method. Because GPR is a non-contact, high-speed, and continuously-measuring method, it has a prosperous future. To study the feasibility of the method, initially it was proven that there was a correlation between the elastic and electrical properties of pavement materials.

Lab experiments revealed a close relation between the dielectric constant of asphalt and its density. Both FMCW and Pulse GPR were used to measure the dielectric constant for different densities, and the results showed a monotonic correspondence between the dielectric constant and density of asphalt.

Furthermore, the field tests were performed using the Pulse GPR to find the correlation between pavement deflection and GPR data. The FWD was used to measure the pavement deflection. Once the correlation was found, the GPR was used to estimate the pavement deflection. Then, the estimated results were compared with the FWD results. The estimated and measured pavement deflections were close and within an acceptable error. However, these correlations were not measured in conjunction. In the case of actual pavements, there are several pavement layers involved, including the asphalt surface, base, sub-base and sub-grade. Even though the correlation between the dielectric constant and asphalt density should ideally remain the same, the pavement deflections are not entirely occurring, due to the top asphalt layer. If the pavement structure used for mapping the correlation between the FWD and the GPR is different than the structure on which the actual measurements are done, the correlation is relatively weaker.

The GPR would still prove to a good method for preliminary determination of non-homogenous patches in longer pavement sections. Once these non-homogenous patches are marked using the GPR, the FWD can be used only on those patches to find

the anomalies in the elastic properties of pavements. This process would be very useful in saving the man hours put into the measurement of elastic properties of pavements for maintenance purpose.

Future work on the same line would be a consideration for the formation of a database of similar correlations for various kinds of pavement structures. This database of correlations shall be used for high-speed GPR measurements on the pavements with known structures to further study the effect of deeper pavement layers on the GPR results.

References

[1]   R. Caracciolo, A. Gasparetto, and M.Giovagnoni. "Measurement of the isotropic dynamic Young's modulus in a seismically excited cantilever beam using a laser sensor.**"** *Journal of Sound and Vibration*, Vol. 231, No. 5, pp. 1339-1353, April 2000.

[2]   T.Chung, C. Carter, T. Masliwec, and D. Manning. "Impulse Radar Evaluation of Concrete, Asphalt and Waterproofing Membrane." *IEEE Transactions of Aerospace and Electronic Systems*, Vol. 30, No. 2, pp. 404-415, April 1994.

[3]   T. Saarenketo. "Ground penetrating radar Technique in Asphalt Pavement Density Quality Control." GPR 1998 Proc., Kansas.

[4]   http://www.utexas.edu/research/ctr/pdf_reports/1422_3F.pdf

[5]   http://www.wsdot.wa.gov/biz/mats/pavement/fwd.htm

[6]   http://www.official-documents.co.uk/document/deps/ha/dmrb/vol7/section3/hd2994c.pdf

[7]   Y. Chen. "Integrated Laser 2-D Surface Imaging System for Thickness Measurement of Thermoplastic Pavement Marking Materials." Ph.D. dissertation, Electrical and Computer Engineering Department, University of Houston, May 2005.

[8]   S. Darayan, C.Liu, L. C. Shen, and D. Shattuck. "Measurement of electrical properties of contaminated soil." *Geophysical Prospecting*, Vol. 46, No. 5, pp. 477-488, 1998.

[9]   C. Liu and Q. Zou. "A simplified Fourier series expansion method for computing the effective dielectric constant of a two-component, three-dimensional composite material with geometric symmetry." *Modeling and Simulation in Materials Science*, Vol. 4, pp. 55-71, 1997.

[10]   C. Liu and H. Wu. "Computation of the effective dielectric constant of a two-component, three-dimensional composite materials using simple poles." *Journal of Applied Physics*, Vol. 82, No. 1, 1997.

[11]   K. Z. Hu and C. Liu. "Theoretical study of the dielectric constant in porous sandstone containing rock grains, oil and water." *IEEE Transactions on Geosciences and Remote Sensing*, Vol. 38, No.3, pp. 1328-1336, 2000.

[12]   X. Zhao, C. Liu, and L. Shen. "Numerical Analysis of a TM010 Cavity for Dielectric Measurement." *IEEE Transaction on Microwave Theory and Techniques*, Vol. 40, No. 10, pp. 1951-1959, October, 1992.

[13]   C. Liu, J. Li, X. Gan, H. Xing, and X. Chen. "New Model for Estimating the Thickness and Permittivity of Subsurface Layers from GPR Data." *IEE Proc. – Radar, Sonar and Navigation*, Vol. 149, No. 6, pp. 315-319, December 2002.

.

[14]   J. Li, H. Xing, X.Chen, Y.Sun, C. Liu, H. Chen, E. Oshinski, M. Won, and G. Claros. "Extracting rebar's reflection from measured GPR data.**"** Proceedings of the Tenth International Conference on Ground Penetrating Radar, Vol. 1, pp. 367-370, June 2004.

[15]   H. Xing, J. Li, X. Chen, Y. Sun, C. Liu, H. Chen, E. Oshinski, M. Won, and G. Claros. "GPR reflection position identification by STFT." Proceedings of the Tenth International Conference on Ground Penetrating Radar, Vol. 1, pp. 311-314, June 2004.

[16]   E. Fernando, W. Liu, and B. Dietrich. "Computer Program for Network Level Determination of Pavement Layer Thicknesses." Proceedings of the International Conference on Ground Penetrating Radar, June 2002.